PHOTOCATALYTIC NANOCOMPOSITES FOR INCREASED OPTICAL ACTIVITY

A THESIS
SUBMITTED TO THE DEPARTMENT OF PHYSICS
AND THE INSTITUTE OF ENGINEERING AND SCIENCES
OF BILKENT UNIVERSITY
IN PARTIAL FULLFILMENT OF THE REQUIREMENTS
FOR THE DEGREE OF
MASTER OF SCIENCE

By
Sümeyra Tek
January 2008

I certify that I have read this thesis and that in my opinion it is fully adequate, in scope and in quality, as a thesis for the degree of Master of Science.

Assist. Prof. Dr. Hilmi Volkan Demir (Supervisor)

I certify that I have read this thesis and that in my opinion it is fully adequate, in scope and in quality, as a thesis for the degree of Master of Science.

Assist. Prof. Dr. Tuğrul Senger

I certify that I have read this thesis and that in my opinion it is fully adequate, in scope and in quality, as a thesis for the degree of Master of Science.

Assist. Prof. Dr. Dönüş Tuncel

Approved for the Institute of Engineering and Sciences:

Prof. Dr. Mehmet B. Baray
Director of Institute of Engineering and Sciences

ABSTRACT
PHOTOCATALYTIC NANOCOMPOSITES FOR INCREASED OPTICAL ACTIVITY

Sümeyra Tek
M.S. in Physics
Supervisor: Assist. Prof. Dr. Hilmi Volkan Demir
January 2008

To combat environmental pollution, photocatalytic decomposition provides degradation of organic and inorganic contaminants near the surface of the photocatalyst nanoparticles by converting optical energy of the absorbed light into chemical energy for the redox reactions. However, photocatalytic activities of such semiconductor metal-oxide nanoparticles are limited with their bandgap energy that allows for optical absorption typically in the ultraviolet spectral range. Yet another limitation is that the photocatalytic activity of these semiconductor nanoparticles is substantially reduced when they are immobilized in solid thin films, resulting from their effectively decreased active surface area. But such immobilized nanoparticles are much more desired in industrial applications, e.g., for mass environmental decontamination and outdoors/indoors self-cleaning on large surfaces. To address these issues, in this thesis, we investigated and demonstrated the spectral behavior and time evolution of optical activity curves of immobilized TiO_2 and ZnO nanoparticles. We studied the nanoparticle size effect for the optical activity and demonstrated significant increase in the resulting photocatalysis with decreasing the size of such immobilized nanoparticles for the first time. We obtained optimal excitation conditions for TiO_2 and ZnO nanocomposite films separately. We achieved

maximum optical recovery levels of 93% for TiO_2 nanoparticles and 55% for ZnO nanoparticles at the excitation wavelengths of 310 nm and 290 nm, respectively, after optical irradiation with an excitation density of 7.3 J/cm^2, where we observed no optical recovery for their respective negative control groups (with no nanoparticles). In these comparative spectral studies, we showed strong correlation between the differential optical recovery and the photocatalytic activity. For further substantial enhancement in the near ultraviolet and visible spectral ranges, we also proposed and demonstrated the use of a unique combination of TiO_2-ZnO nanoparticles integrated together into the same resin. In this novel approach, we observed higher levels of photocatalytic activity under optical irradiation at and above 380 nm compared to the cases of only TiO_2 or only ZnO nanocomposite films with the same total metal-oxide nanoparticle density. At 400 nm in the visible, we accomplished an optical recovery level of ~30% with the combination of TiO_2-ZnO nanoparticles together while this level was only ~14% for the TiO_2 nanoparticles alone and ~3% for the ZnO nanoparticles alone under identical conditions. Even at 440 nm, we obtained ~20% optical recovery using the TiO_2-ZnO photocatalytic synergy, despite the optical activity of the single type of nanoparticles alone close to the zero base-line of their control group. These proof-of-concept experimental demonstrations indicate that such TiO_2-ZnO combined nanocomposite films hold great promise for efficient environmental decontamination in daylight.

Keywords: Nanoparticles, nanocomposite films, TiO_2, ZnO; optical recovery, ultraviolet, visible; photocatalytic synergy; photocatalysis, environmental decontamination.

ÖZET

ARTIRILMIŞ OPTİK ETKİNLİK İÇİN FOTOKATALİTİK NANOKOMPOZİTLER

Sümeyra Tek
Fizik Bölümü Yüksek Lisans
Tez Yöneticisi: Yrd. Doç. Dr. Hilmi Volkan Demir
Ocak 2008

Çevre kirliliği ile mücadele etmek için, fotokatalitik ayrıştırma fotokatalizör nanoparçacıklarının soğurdukları ışığın optik enerjisini redoks tepkimelerinde kullanılmak üzere kimyasal enerjiye çevirerek yüzeylerinin yakınındaki organik ve inorganik birikintilerin parçalamasını sağlar. Ancak, bu yarı-iletken metal-oksit nanoparçacıkların fotokatalitik etkinlikleri, yasak enerji aralıklarının sadece mor ötesi ışık tayfında optik soğurmaya izin vermesiyle sınırlanmaktadır. Başka bir sınırlama da bu nanoparçacıkların katı ince bir film içerisine sabitlendiklerinde toplam aktif yüzey alanındaki ciddi azalmaya bağlı olarak fotokatalitik etkinliklerinin ciddi bir şekilde düşmesidir. Fakat bu türden sabitlenmiş nanoparçacıklar endüstriyel uygulamalarda (örneğin, geniş çaptaki çevresel temizlenme ve geniş yüzeylerin kendiliğinden iç/dış temizlenmelerinde) çok daha caziptir. Bu konuları hedef alarak, bu tezde, sabitlenmiş TiO_2 ve ZnO nanoparçacıklarının optik etkinlik eğrilerinin spektral davranışlarını ve zamanla olan gelişimlerini inceledik ve gösterdik. Optik etkinlikte nanoparçacık boyutunun etkisini çalıştık. Sabitlenmiş nanoparçacıkların boyutunun küçültülmesiyle fotokatalizde meydana gelen ciddi artışı ilk defa gösterdik. TiO_2 ve ZnO nanokompozit filmlerinin herbiri için ayrı ayrı optimal uyarma koşullarını elde ettik. 7.3 J/cm^2 uyarma yoğunluğundaki optik ışığa maruz tutulmaları neticesinde TiO_2 nanoparçacıkları için %93 ve

ZnO nanoparçacıkları için %55 maksimum optik geri kazanımlara ulaştık. TiO_2 ve ZnO için maksimum optik geri kazanımları sırasıyla 310 nm ve 290 nm uyarılma dalgaboylarında elde ettik. Aynı optik uyarılma neticesinde ise, nanoparçacık içermeyen negatif kontrol gurubunda herhangi bir optik geri kazanım gözlenmedi. Bu spektral karşılaştırmalı çalışmalarımızda, diferansiyel optik geri kazanım ve fotokatalitik etkinlik arasında güçlü bir uyumluluk gözlendi. Yakın mor ötesi ve görünür bölge tayfında fotokatalitik etkinliğin artırılması için TiO_2-ZnO nanoparçacıklarının tek bir kombinasyonunun aynı reçine içine entegrasyonunu önerdik ve deneysel olarak gösterdik. Bu alışılmamış yaklaşımla, 380 nm ve üzerindeki uyarılma dalgaboylarında, aynı toplam metal-oksit nanoparçacık konsantrasyonuna sahip sadece TiO_2 ve sadece ZnO nanokompozit filmlerine nazaran daha yüksek değerlerde fotokatalitik etkinlik gözlemledik. Sadece TiO_2 içeren nanokompozit film için %14 ve sadece ZnO içeren nanokompozit film için %3 optik geri kazanım değerlerinin elde edildiği görünür bölge 400 nm uyarılma dalgaboyunda TiO_2-ZnO nanoparçacık kombinasyonuyla aynı şartlarda %30 civarında optik geri kazanım sağladık. TiO_2-ZnO fotokatalitik sinerji etkisi sayesinde tek tip nanoparçacık filmlerinin optik etkinliğinin fotokatalizör kullanılmayan kontrol filminin sıfır tabanına yakın olduğu 440 nm uyarılma dalgaboyunda dahi %20'lere varan optik geri kazanım elde ettik. İlk deneysel ispatı olan bu sonuçlar, TiO_2-ZnO birlikte olduğu nanokompozit filmlerinin güneş ışığında verimli fotokatalitik çevresel temizlenme için kullanımını gösteriyor.

Anahtar Sözcükler: Nanoparçacıklar, nanokompozit film, TiO_2, ZnO; optik geri kazanım, mor ötesi, görünür bölge; fotokatalitik sinerji; fotokataliz, çevresel temizlenme.

Acknowledgements

I would like to express my deepest appreciation to my supervisor, Asst. Prof. Dr. Hilmi Volkan Demir for his motivation and technical support since my undergraduate years. I am greatly indebted to his assistance and understanding in matters of non-academic social life related concerns in addition to his scientific guidance and encouragement at all stages of my work.

I would also like to thank my committee members, Assist. Professor Dr. Tuğrul Senger and Assist. Professor Dr. Dönüş Tuncel, for their valuable comments and suggestions.

I would like to extend my thanks to our research partners, Gülsen Çeliker and Dilek Yücel, from DYO for providing samples, useful discussions, and great hospitality during my internship at DYO in Izmir.

I would like to thank İbrahim Murat Soğancı, Evren Mutlugün, İlkem Özge Huyal and Dr. Nihan Kosku Perkgöz for their contributions to this thesis and being very good friends of mine.

I would also like to acknowledge Prof. Dr. Ekmel Özbay for the facilities that we share at Nanotechnology Research Center. I would like to thank Advanced Research Laboratory researchers and staff, especially Murat Güre and Ergün Karaman.

I would like to thank Demir Group members for their great friendship: Sedat Nizamoğlu, Tuncay Özel, Rohat Melik, Can Uran, Emre Sarı, Aslı Koç, Emre Ünal, Gülis Zengin and Özgün Akyüz.

I would like to thank my home-mate Özlem Yeşilyurt, and my friends from Physics Department: Selcen Aytekin, Sinem Binicioğlu Çetiner, Ceyda Sanlı, and Bahar Kop.

My greatest gratitude goes to all my family: my parents, my sisters, especially Zeynep Betül, and my parents-in-law for all their support.

Finally, I would like to thank my love Süleyman for his understanding, encouragement, and endless love; he is always there where I need him. This thesis is dedicated to him.

Table of Contents

List of Figures

List of Tables

Chapter 1

Introduction

In 1972, Fujishima and Honda discovered the photocatalytic splitting of water on TiO_2 electrodes [1]. This discovery opened a new research area in heterogeneous photocatalysis. Chemists, physicists, and engineers have thus far conducted various research studies on this subject. Early studies were mainly focused on the energy renewal and storage [2-4]. The production of renewable and nonpolluting fuels by using hydrogen evolution from water splitting on the photocatalysts are still attractive [5]. In recent years, photocatalyst semiconductors have also become increasingly attractive for their peculiar optical properties in decontamination of large media.

Photocatalyst semiconductors offer solution to the reduction of environmental and biological pollution. Today the alarmingly rapid increase in the amount of CO_x has become one of the most important problems threatening the world. Similarly, the equally rapid increase in the amount of NO_x in the atmosphere and water is yet another problem that the world faces. Photocatalysts provide remedies for the degradation of CO_x and NO_x amounts in the medium through redox reactions with the use of light [6, 7]. Photocatalysts also present solution for the decomposition of biological species such as harmful fungi, viruses and bacteria. Such harmful species are decomposed into harmless inorganics with the use of photocatalysts [8].

The size of a photocatalyst is an important parameter affecting the efficiency of the photocatalytic degradation process. In particular, their efficiency is increased when the size is changed from bulk to their nanoparticle dimensions [9-11]. Most of the recent research thus target synthesizing nanoparticle size semiconductor photocatalysts and increasing their photocatalytic activities. Photocatalytic nanoparticles that are immobilized in solid thin films are more convenient for industrial applications. Many studies have been carried out in

solid thin films or aqueous solutions where nanoparticles are not immobilized. In this case, the removal of the photocatalyst itself from the medium following the decontamination process is not easy [12]. One possible solution to overcome this problem is to immobilize the nanoparticles on a suitable substrate [13, 14]. To date there is comparatively much less research work is conducted on immobilized photocatalyst nanoparticles. In our research, the photocatalytic nanoparticles are immobilized through chemical integration of the nanoparticles into three dimensional host resins. This approach allows for a better homogenous distribution of the nanoparticles with low number of aggregates to compete with the decreased activity due to their immobilization. Very high photocatalytic activities achieved with increased surface to volume ratios of nanoparticles for the reactions occurring at the surface of the photocatalyst.

Utilization of solar light is important for decontamination of large outdoor areas. Highly active photocatalytic nanoparticles such as TiO_2 and ZnO are wide bandgap semiconductors that limit the degradation of pollutants under sunlight. These nanoparticles can absorb ultraviolet light at wavelengths shorter than ~388 nm. However UV content of the solar light is only a small percent (~7%) of the whole solar spectrum. Our motivation in this thesis is to make the photocatalytic activity possible with the visible content of sunlight, by extending the photocatalytic activity of our nanocomposite films into the visible. For this purpose, we embedded TiO_2 and ZnO nanoparticles into the same resin through chemical integration. We investigated the optical spectral behavior of those nanocomposite films by activating them at selected wavelengths and analyzing their photocatalytic activities at those wavelengths. In this thesis, we focus on increasing the photocatalytic activity of immobilized nanoparticles (TiO_2 and ZnO nanocomposite films) in UV, we present their optical characterization and proposed solution of TiO_2-ZnO combined nanocomposite films for enhanced photocatalytic activity in the near UV and the visible.

The organization of this thesis is as follows. In the second chapter, the photocatalytic materials and the mechanism of photocatalysis are introduced.

The common use of photocatalytic materials and the parameters affecting photocatalysis are discussed. In the third chapter, we focus on nanostructured photocatalysts, particularly TiO_2 and ZnO nanoparticles, and their immobilization in thin films. In the fourth chapter, the experimental procedure and characterization are provided. Experimental results are demonstrated and discussed in the fifth chapter.

The research work of this thesis is carried out as a part of close collobration between the Demir Lab (Devices and Sensors Research Group) of Bilkent University and the R&D Lab (G. Celiker and D. Yucel) of DYO, Yasar Holding.

In the beginning, the size effect on photocatalytic activity of TiO_2 nanocomposite film is shown, which was not reported before for the immobilized forms through chemical integration. Also effect of recontamination and reactivation is reported. The results of this section are submitted for publication [15]. Then, optical spectral response and comparative photocatalytic activity studies are provided. The results of this section are published in Journal of Nanophotonics [16]. At the end of this chapter, we show the promising optical recovery levels achieved with the use of combined nanocomposite film for enhanced photocatalytic activity under sunlight. The results of this section are used in patent application and our submission for publication. In the last chapter, we conclude our photocatalytic research work with a summary of the highlights of the previous chapters.

Chapter 2

Background On Photocatalysis

2.1 Photocatalysts

Semiconductor solids that promote chemical reactions in the presence of light without being consumed are known as photocatalysts. To be a good photocatalyst the semiconductor material should be photoactive, non-toxic, and photostable and should offer the ability to be photocatalytically activated under sunlight. TiO_2, ZnO, WO_3, CdS, ZnS, $SrTiO_3$, SnO_2, WSe_2, Fe_2O_3, etc. are among semiconductor solids used as photocatalysts [17]. The range of the optical spectrum where these semiconductor metaloxides are activated is important to determine whether or not the optical activation is possible under sunlight. Semiconductors with superior photocatalytic properties are those with wide bandgaps such as TiO_2 and ZnO. Their photocatalytic performance is determined through the process of optical absorption of the incident photons in the UV, and subsequent photogeneration of electron-hole pairs that exhibit dissimilar parity in the respective conduction and valence bands, leading to low recombination rates [8]. On the other hand, a high photocatalytic activity in daylight can be achieved with photocatalysts that have bandgap energies smaller than 3 eV to cover a significant part of the solar spectrum but small bandgap semiconductors have low photoactivities [18].

2.2 Process underlying behind photocatalysis

Degradation of many pollutants, especially organic ones, on the surface of a photocatalyst is promoted in the presence of oxygen and water, with incident light having photon energies larger than the bandgap energy of semiconductor photocatalyst.

The photons absorbed in the photocatalyst excite the electrons from the valence band to the conduction band of the semiconductor photocatalyst, producing electron-hole pairs. Following optical absorption of light, two reactants are adsorbed on the surface of the photocatalyst. They are reduced and oxidized. These reactions are allowed by the band energy position of semiconductor and the redox potentials of the adsorbates. In the reduction mechanism, the redox potential of the adsorbate (acceptor) is below the conduction band of the semiconductor. Excited electron is transferred from the conduction band to the adsorbed particle. In the oxidation mechanism, the redox potential of the adsorbate (donor) is above the valence band of the semiconductor to donate an electron to the vacant hole in the valence band. Oxygen and water are the adsorbates in the photocatalytic reactions [8].

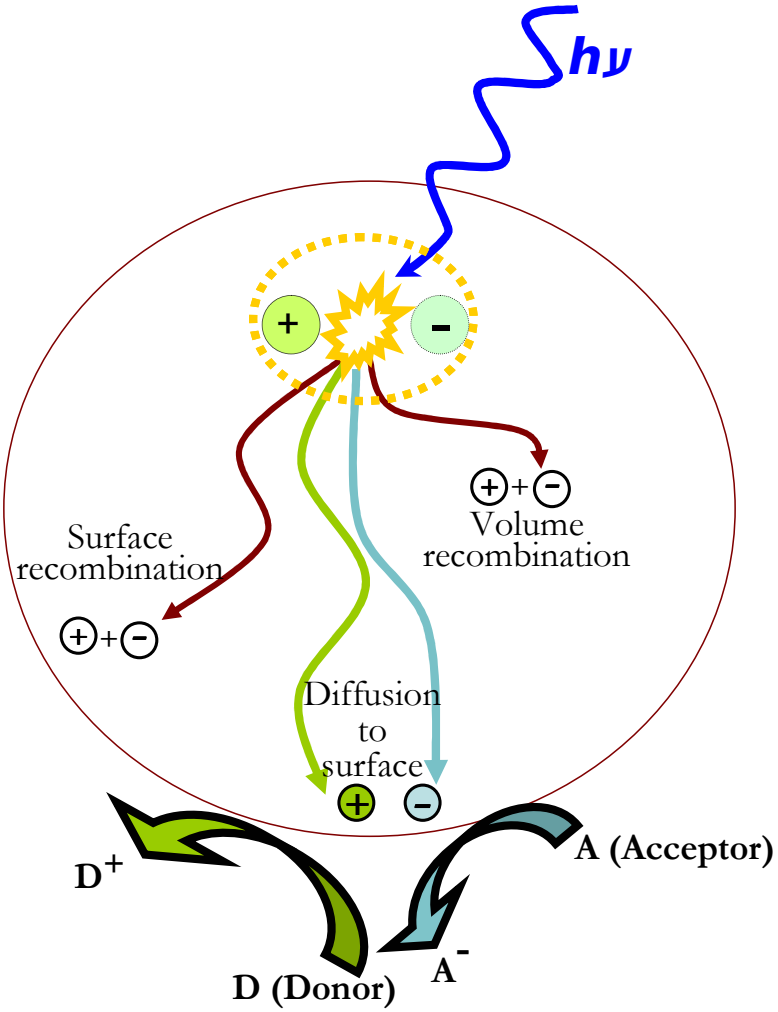

Figure 2.2.1 Schematic photoexcitation of the semiconductor photocatalyst and the following redox reactions.

The mechanism of photocatalysis is illustrated in Fig. 2.2.1. There are four processes that may occur after the absorption of light. Electron-hole pair either recombines or migrates to the surface leading to oxidation and reduction of the adsorbates. Recombinations can occur at the surface or within the bulk of the photocatalyst. Thus, upon optical irradiation, there is a sufficient lifetime for the electron-hole pair for the charge transfer to the adsorbed species on the surface of the semiconductor. This lifetime is in the regime of nanoseconds [19]. In the absence of such acceptor and donors, electron-hole pair recombines within a few nanoseconds [8, 17].

In presence of water and oxygen, a chain of reactions occur. Water is oxidized by positive holes and oxygen is reduced by the photoelectron of the conduction band. Reactive oxygen species such as H_2O_2, $^{\cdot}O_2^-$, and hydroxyl radical $^{\cdot}OH$ are produced. The reactions that are promoted with the absorption of photon (hυ) are given below [8].

Semiconductor (SC) + hυ → SC ($e^- + h^+$) (1)

The reactions that are initiated with conduction band electron (e^-) are given as follows

$SC(e^-) + O_2 \rightarrow SC + {}^{\cdot}O_2^-$ (2)

$SC(e^-) + {}^{\cdot}O_2^- + 2H^+ \rightarrow SC + H_2O_2$ (3)

$SC(e^-) + H_2O_2 \rightarrow SC + {}^{\cdot}OH + OH^-$ (4)

${}^{\cdot}O_2^- + H_2O_2 \rightarrow {}^{\cdot}OH + OH^- + O_2$ (5)

${}^{\cdot}O_2^- + H^+ \rightarrow {}^{\cdot}HO_2$ (6)

$SC(e^-) + {}^{\cdot}HO_2 \rightarrow SC + HO_2^-$ (7)

$HO_2^- + H^+ \rightarrow H_2O_2$ (8)

$2\ {}^{\cdot}HO_2 \rightarrow O_2 + H_2O_2$ (9)

The reactions that are initiated with valence band hole (h^+) are given as follows

$SC(h^+) + H_2O_{(ads)} \rightarrow SC + {}^{\cdot}OH_{(ads)} + H^+$ (10)

$SC(h^+) + 2H_2O_{(ads)} \rightarrow SC + 2H^+ + H_2O_2$ (11)

$SC(h^+) + OH^-_{(ads)} \rightarrow SC + {}^{\cdot}OH_{(ads)}$ (12)

The resulting highly reactive oxygen species (such as H_2O_2 and $^{\cdot}O_2^-$) and hydroxyl radical ($^{\cdot}OH$) attack the organic contaminants on the surface leading to degradation. Thus optically illuminated photocatalyst semiconductor can degrade and mineralize organic compounds through a series of oxidation reactions [8].

2.3 Early studies in photocatalysis

TiO_2 has been used in industry as white pigments since ancient times. Its photoactivity was observed first as the flaking of paints and degradation of fabrics including TiO_2. In 1938, photobleaching of dyes under UV irradiation was reported. The term 'photocatalyst' was not used for TiO_2 in those times; instead used the term 'photosensitizer' [20]. In 1960s, photochemical power of TiO_2 was studied. Photocatalytic splitting of water on TiO_2 electrodes was discovered in 1972, by Fujishima and Honda [1]. In 1980s many studies were conducted on hydrogen production through TiO_2 photocatalysis. Various semiconductors were explored for better utilization of solar light for hydrogen production. But they were not as more efficient and stable as TiO_2. Subsequently, the direction of research turned into the decontamination of organic pollutants [20]. In recent years many scientists including chemists, physicists, and engineers have worked for enhancing photocatalytic efficiencies of semiconductors for decontamination of large indoor and outdoor areas.

In 1990s, one of the first commercialized self-cleaning surfaces was TiO_2 coated cover glass for tunnel light. In most tunnels in Japan, contamination of cover glass of tunnel lamps with exhaust particles was a serious problem. It caused a significant decrease in the illumination power of lamp emitting through the cover glass. High pressure sodium lamps that have UV content of about 3 mW per cm^2 at a position of its cover glass were used. UV light is used to clean cover glass coated with photocatalyst [21]. Its photograph is given in Fig. 2.3.1.

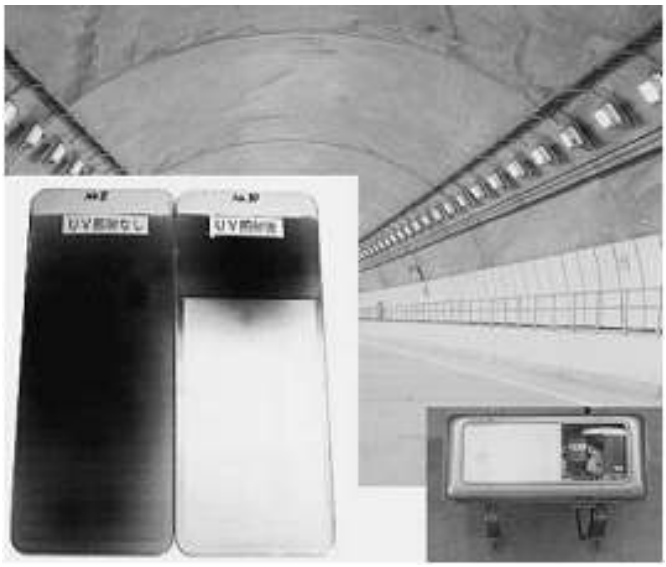

Figure 2.3.1 Glass covers on tunnel lighting lamps contaminated by automobile exhaust without TiO_2 and maintained clean with TiO_2 coating (after [21]).

Banerjee showed the anti-bactericidal activity of TiO_2. Gram negative *pseudomonas* was used as the testing bacterial colony, which is known as the major colonizer of freshwater biofilms. Atomic force microscope image belonging to existing bacterial colony was observed to be smooth after exposed to near-UV light [8]. One of the applications of photocatalytic decomposition of microorganisms was conducted by Sunada. *Escherichia coli* cells on the surface of metal-oxide can be completely decomposed in a week under the activation of UV of 1 mW/cm^2 [22].

Such photocatalytic metal-oxides find a wide range of applications including prevention of air pollution by reducing NO_x and CO_x amounts in air [6, 7]. Especially immobilized form of the most commonly used photocatalysts, TiO_2 and ZnO, are promising with their high photocatalytic activities. Nanosized metal-oxides show extremely high photocatalytic efficiencies with their high surface to volume ratios and superior properties with smart applications of thin films [15, 16].

Studies that have been conducted so far showed that photocatalytic degradation can be applied to all kinds of organic and inorganic pollutants including heavy metals [17].

2.4 Parameters affecting photocatalysis: adsorption, intensity of light, pH, size, surface properties, and activation wavelength

Degradation mechanism takes place on the surface of the photocatalyst. The concentration of the adsorbate directly affects the photocatalytic degradation rate of the pollutants to be degraded [23, 24]. Photocatalytic degradation rate is linearly dependent with light intensity at low intensities. It depends on the square root of light intensity for medium intensities. At high intensities photocatalytic degradation rate is independent of the intensity of light [25, 26].

The effect of pH on photocatalytic degradation varies due to the kind of semiconductor used and the kind of adsorbed pollutant [27]. Increasing or decreasing pH affects the adsorption of the pollutant and thus, the degradation rate. pH affects the surface charge of the photocatalyst and the ionizability of the pollutant. Adsorption is enhanced at lower pH values. Strongly adsorbed pollutants degrade faster. At higher pH values above pH 9, degradation rate is also enhanced due to the increased OH^- anions on the photocatalyst surface. Therefore all these rates depend on the type of catalyst and the adsorbed pollutant [23, 28, and 29].

The particle size of photocatalysts is an important parameter that affects photocatalytic activity. Decreasing the size of the catalyst, surface to volume ratio is increased, thus photocatalytic activity is increased. Nanosized semiconductors are widely used for their superior photocatalytic properties [15, 16].

The surface properties of semiconductor photocatalysts also affect the photocatalytic activity. It was shown that surface morphology and crystal structure have a direct effect on the photocatalytic activity of TiO_2 sol-gel films. Heat treatment can modify crystal structure leading to an increased photocatalytic activity [30].

The degradation mechanism is promoted with the absorption of light by the semiconductor photocatalyst. In optical activation, electrons are excited from the valence band to the conduction band leading to e-h pair formation. The photon energy of the incident light should be above the band gap energy of the semiconductor. So activation wavelength is an important parameter for the photocatalytic reactions. Most commonly used photocatalysts are wide band gap semiconductors that can be activated in UV light. However electromagnetic radiation of sun has only 7% UV content that strikes the atmosphere, which decreases more during penetrating the atmosphere [31]. According to Sasaki [32], the UV part of solar radiation detected on the Earth in 1990-1992 was not more than 0.145% at 290-320 nm and 4.1% at 320-400 nm.

2.5 Nanosized materials

Many properties of photochemical processes change as the semiconductors change scale from bulk to nanorange. Nanosized semiconductors exhibit special thermodynamic, magnetic, photochemical, photo-physical, and electro-physical properties. When semiconductors are in the nanoscale regime, their size has significant effects on their properties. Changing the size of such semiconductor nanoparticles opens up the opportunity to control their characteristics [33].

Varying semiconductor nanoparticle size strongly affects the semiconductor-light wave interaction and the resulting processes. These processes depend on the optical absorption of light, dynamics of photo-generated exciton, the

consequences of electron-hole recombination, and the photo-chemical reactions in the presence of reagents adsorbed on the semiconductor surface [34].

The size effects in semiconductor nanoparticles can be divided into two. The first one is the result of increased surface to volume ratio and change in surface roughness is observed in semiconductor nanoparticles of 10-100 nm in size. The other is the change in the electronic state of the semiconductor due to the quantum size effects dominating especially below a critical size (~10 nm) at room temperature. The critical size, which is the threshold for the quantum size effects, differs for different semiconductors, depending on the chemical structure of the nanoparticle. It is comparable to the De Broglie wavelength of the free electron [35].

2.6 Nanoparticle semiconductors in photocatalysis (surface area, band gap properties, and absorption)

A series of significant changes in the characteristics of semiconductor when reduced to a small size comparable to the delocalized exciton depend on the radius of nanoparticle R and the bohr exciton radius a_B. In $R \geq a_B$ regime, the electronic structure of semiconductor is the same as of the bulk. In strongly confined regime where $R < a_B$, semiconductor has discrete energy levels with an increase in the forbidden gap of the semiconductor i.e., widening of its bandgap. The change in the electronic properties of semiconductor results in a shift in the optical absorption edge to shorter wavelengths due to the widening of the bandgap. On the other hand, small size enhances the probability of the charge carriers to escape to the surface of the semiconductor. The recombination of electron-hole pair and the photochemical charge transfer reactions to the adsorbates on the surface of semiconductor are competing processes for the case of photocatalysis [33].

Semiconductor nanoparticles are characterized with their extremely short time for the diffusion of the excited charges from the volume of the nanoparticle to its surface where adsorbate is close enough to permit the electron tunneling. For the case of TiO_2 of 10 nm in size, the time for an electron to escape to the surface is smaller than 10 ps. Direct electron-hole recombination time for TiO_2 is in the range of 100 ns [33]. Thus nanostructured semiconductor photocatalysts have enhanced photocatalytic activities in the presence of light corresponding to energies larger than the forbidden energy gap.

The potentials of valence and conduction bands play an important role during photocatalytic reactions. The potential level of the conduction band in the semiconductor should be above the reduction potential of the acceptor and the potential level of the valence band should be below the oxidation potential of the donor (for Normal Hydrogen Electrode scale) [36]. Quantum confinement results in a displacement of conduction band to the more negative region of the electrochemical scale of potential, and valence band to the more positive region. The increase in the absolute values of potentials of the photogenerated charges increases the photocatalytic activity of the semiconductor nanoparticles.

2.7 TiO_2 and ZnO nanoparticles

Among various semiconductors, TiO_2 and ZnO are the most commonly used photocatalysts especially employed for the degradation of several environmental contaminants with their high photosensitivity, stability, and large band gaps [37]. TiO_2 is also chemically inert and non-toxic that can be used in a wide range of applications [38]. To describe their photocatalytic activities, one should look into the electronic energy band structure of TiO_2.

TiO_2 is a large band gap semiconductor. Its conduction and valence bands are composed of pure 3d orbital of titanium and 2p orbitals of oxygen hybridized

with Ti 3d states, respectively. Under UV light irradiation, electrons in the TiO_2 valence band are excited to the conduction band. The dissimilar parity of the conduction and valence bands causes a reduction in the electron-hole recombination rate to allow the e^--h^+ pair to diffuse to the surface. It is followed by a chain of reactions to produce highly reactive oxygen species and hydroxyl radicals ($^{\bullet}OH$) that are powerful indiscriminate oxidizing agents. Similarly, ZnO is a member of the 3d metal-oxide series. As in TiO_2, the photoexcited e^--h^+ pair of ZnO has also dissimilar parity, making ZnO a good candidate for photocatalyst. ZnO and TiO_2 are differed from the other 3d transition metal-oxide semiconductors with their stability upon photoexcitation [8].

2.8 Immobilization in thin films

To date, most of the applications of photocatalytic decomposition are reported to be conducted in aqueous media. This, however, gives rise to technical difficulties associated with the removal of photocatalyst from the medium and their use in wide-scale industrial applications. To circumvent these issues, one remedy is to immobilize the photocatalyst in thin films on a suitable substrate. But the immobilization then leads to the reduction in the active catalyst surface area (and thus in the photocatalytic activity). To compensate for this reduction in the photocatalytic activity, though, nanoparticle can be utilized to effectively increase the active surface area provided that these nanoparticles are integrated into the thin film properly and well dispersed [16].

Immobilization can be achieved through the integration of photocatalytic nanoparticles inside three dimensional host resin via solgel route. Nanoparticles are then well dispersed in the three-dimensional solgel matrix through full chemical integration for highly efficient environmental decontamination.

Highly active photocatalysts such as TiO_2 also cause decomposition of their organic host in the presence of UV light, which is called chalking for the case of

paints. To overcome this drawback, TiO_2 is coated by an inert coating such as SiO_2 or Al_2O_3 [39].

In our case, silikon-alkoxides are used for the organic-inorganic material formation, which prevents chalking of the host resin. The sol-gel synthesis of silica is based on the hydrolysis and condensation of silicon-alkoxides, $M(OR)_z$, where R is an alkyl group (R=Me, Et, Pr,…). Hydrolysis gives reactive silanol groups where as condensation leads to the formation of bridging oxygen. Most common silicon alkoxides are $Si(OCH_3)_4$ (tetramethyl ortho silicate) and $Si(OC_2H_5)_4$ (tetraethyl ortho silicate) [39].

Si-OR + H_2O → SiOH + ROH hydrolysis

Si-OH + RO-Si → Si-O-Si + ROH

$Si(OR)_4$ +2H_2O→SiO_2 + 4 ROH (inorganic-organic hybrid) [39]

Chapter 3

Our Experimental Results

Our photocatalytic experiments include transmission measurements of the nanocomposite films at initial state, after contamination, and after activation at selected wavelengths. Important parameters of the experiment are activation wavelength, intensity of light, degree of contamination, and activation time. We have conducted our experiments at different activation wavelengths to obtain the optical spectral response of those photocatalytic films formed with different types of metal-oxide nanocomposites. In all studies we employed monochromatic light for the activation of our films at selected wavelengths in the UV part of the spectrum through a series of experiments. In our recent studies, experiments include activation also in the visible spectrum. These studies, showing the optical spectral response of photocatalyst semiconductors immobilized in films are our recent contributions to the literature where activations are carried out mostly at a single fixed activation wavelength [40] or a UV source including a large spectrum [41, 42] or under direct sunlight [43].

Light intensity is one of the most important parameters for photocatalysis. Light intensity has a direct effect on the reaction rate. Because both the recombination rate of the photo-generated electron-hole pair and the charge transfer at the surface of the photocatalyst depend on light intensity. The electron-hole pair recombination is a second order process when the charge transfer is a first order one. The higher light intensity leads to a relative increase of the recombination rate when compared to the rate of charge transfer [44]. Increased electron-hole recombination with high light intensity also results increasing the temperature of the catalyst, which leads to a decrease in adsorptive capacity [26].

In the literature, the reaction rate is reported to be proportional to the light intensity under low intensities. It is proportional to square root of the light

intensity under moderate light intensities when it is independent of light intensity under high intensities [25, 26, 45-47]. In our experiments, the light intensities we have chosen are in low intensity range so that photocatalytic degradation is proportional to the light intensity. The product of light intensity and activation time is kept constant through the same set of experiments.

The degree of contamination determines the availability of pollutants to be degraded. For achieving more precise results, we applied the same contamination procedure for an equal amount of time to all samples in the same experiment set. Drop casting or spraying methods are used at different experiment sets.

3.1 Photocatalytic Recovery Levels

Photocatalytic recovery levels are obtained from the resulting transmission data of the conducted experiments. One of the activated sample photograph is given in Fig. 3.1.1 for better visualization.

Figure 3.1.1 Photograph of TiO_2 nanocomposite film first contaminated with methylene blue and then exposed to UV irradiation.

Methylene blue is used as the contaminant in all our experiments. It is the standard industrial contaminant that becomes colorless when it is chemically reduced in the presence of photocatalyst. When nanocomposite film is

contaminated with methylene blue, a drop in the transmission spectrum in the visible is observed. Upon irradiation with light in the ultraviolet, the transmission curve returns back to its original characteristic level as the methylene blue is degraded during the continuing activation process. The control group experiments (the host resin without any photocatalyst) are carried out for all the experiments conducted at different activation wavelengths. Methylene blue is not degraded in the absence of semiconductor metal-oxide photocatalyst.

Methylene blue has absorbance peaks in the visible between ~450 nm and ~750 nm. Some photocatalytic activity analyses are performed by using the change in the absorbance of methylene blue due to the decomposition under UV [49, 50]. Methylene blue bleaching may result from the reduction of methylene blue to its leuco form, or if it is oxygenated or decomposed. Remote bleaching cannot be a simple reduction to its leuco form. It is either oxygenated or decomposed, which are irreversible processes [50]. In all our experiments, we do not observe oxidation of the molecular oxygen, so the degradation of methylene blue is due to the photocatalytic decomposition [15].

During our experiments, we used a monochromator (CM 110 Spectral Products) and a Xenon light source for both to activate our samples in UV to visible and to take transmission measurements in the visible with Newport power-meter. Optical analysis of photocatalytic recovery is carried out through contaminating our sample and then activating with a monochromatic light at a known wavelength. After each activation period, transmission measurement of activated sample is taken for optical recovery analyses.

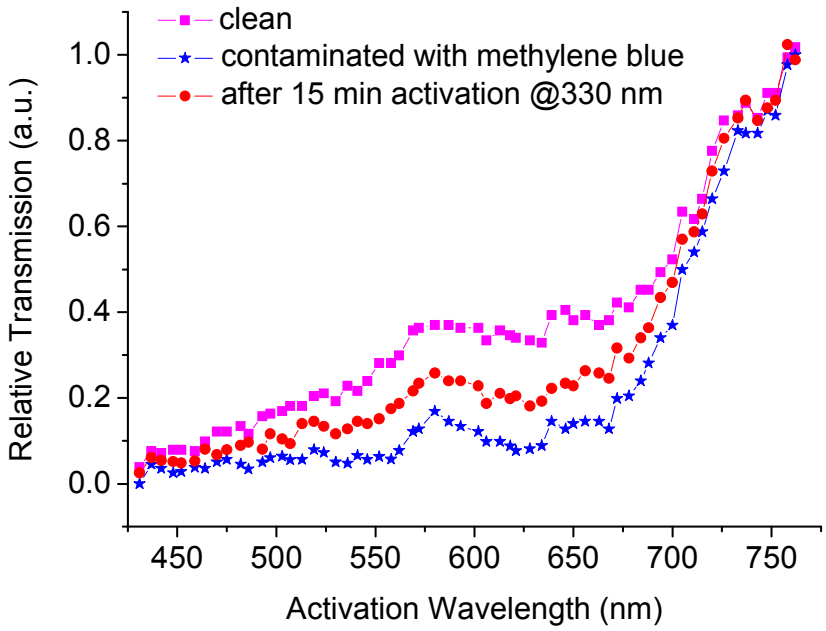

Figure 3.1.2 Optical transmission spectra of TiO_2 nanocomposite film when it is clean, contaminated with methylene blue, and activated with UV light.

Optical recovery level is the ratio of spectral area between activated transmission curve and the contaminated transmission curve of the sample to the area between transmissions of clean and contaminated curves. The optical activation is carried out with a larger slit when transmission is measured through smaller slit of the monochromator. All of the measurements are taken from the same spot within the activated area.

3.2 Size Effect

Till date many studies on photocatalytic activity have been conducted. However most of these experiments were conducted in aqueous solutions. For example, the effect of metal-oxide nanoparticle size was explored for photocatalytic activities only in solutions [51]. The photocatalytic activity in aqueous medium was measured by observing the changes in material concentrations in the

solution which are affected through the photocatalytic decomposition process [15]. However, the size effect studies for immobilized photocatalytic nanoparticles have not previously been studied, which are much more applicable for decontamination of large indoor and outdoor areas. With the use of our optical spectroscopic method for measuring the photocatalytic activity of nanocomposite films, we define a figure of merit for photocatalytic recovery levels for immobilized nanoparticles.

For the experiment sets on the effect of nanoparticle size, TiO_2 (6 nm in diameter) and TiO_2 (21 nm in diameter) are used. Nanoparticles are embedded inside three dimensional acrylic sol-gel matrix. The chemical integration leads to a well dispersed semiconductor metal-oxide nanocomposite with a very low number of aggregates. 6 nm TiO_2 nanocomposite film, 21 nm TiO_2 nanocomposite film, and acrylic sol-gel film (without any photocatalyst nanoparticle) for control experiments are formed.

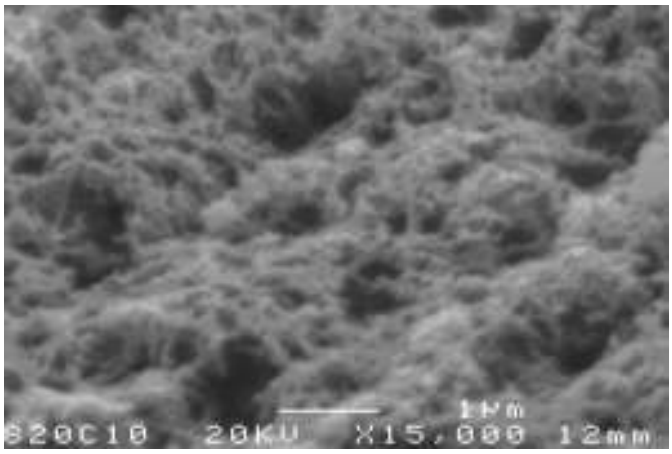

Figure 3.2.1 SEM image of our photocatalytic nanocomposites that nanoparticles are integrated into their three-dimensional sol-gel matrices.

In the experiment, the optical activation wavelength is 330 nm. During experiments, transmission spectra in the visible are measured after every activation periods with constant excitation power density.

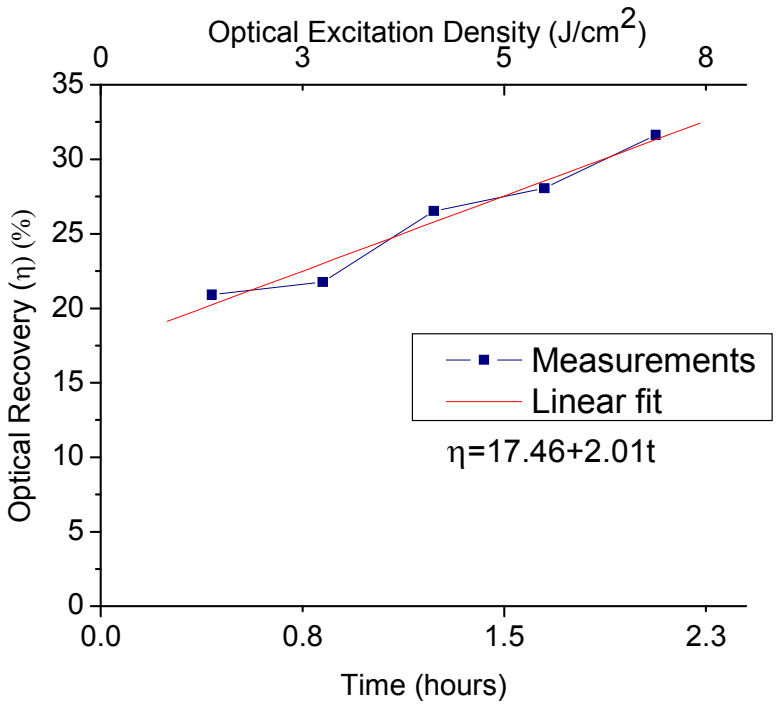

Figure 3.2.2 Optical recovery levels for titanium dioxide nanoparticles (6 nm in diameter) in the early phase of optical excitation process.

Fig. 3.2.2 shows the early phase of photocatalytic activation of 6 nm TiO_2 nanocomposite film under irradiation with 330 nm monochromatic light. The optical recovery is very fast in the early phase of the photocatalytic activation up to the optical activation with 6.88 J/cm^2 [15].

In Fig. 3.2.3, there are five continuing activation durations with optical activation ranging from 10.8 J/cm^2 to 54 J/cm^2. The calculated optical recovery levels after each activation period at 330 nm excitation is obtained for both 6 nm TiO_2 nanocomposite film and 21 nm TiO_2 nanocomposite film. The existing data for early and late phase of activation for 6 nm TiO_2 nanocomposite films show that the degradation of methylene blue is faster in the early phase of activation. The differential optical recovery value (the rate of increase in the photocatalytic recovery) for early phase is 2.01 per hour when it is 0.54 per hour for late phase in which excitation time lasts longer [15].

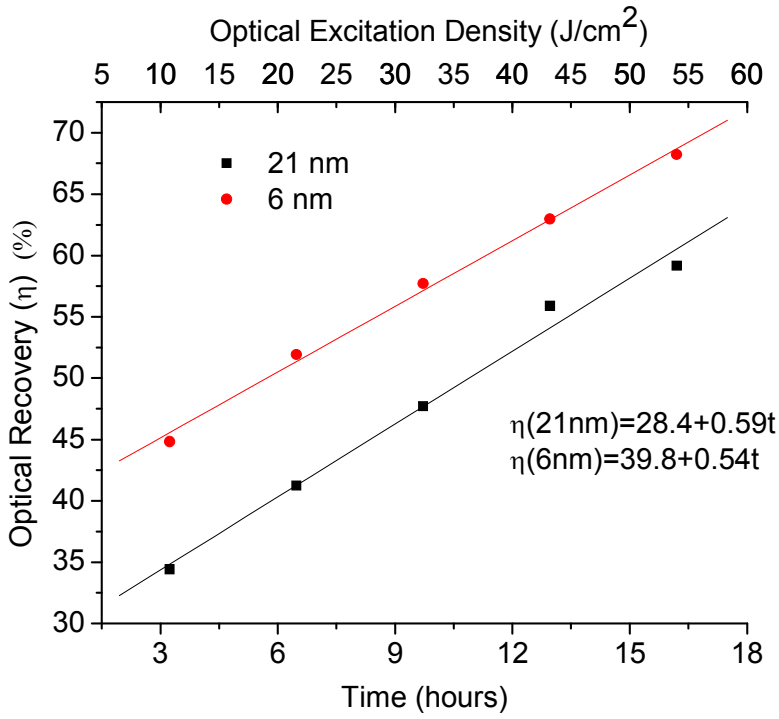

Figure 3.2.3 Optical recovery levels of titanium dioxide nanocomposite films with nanoparticle sizes of 6 nm and 21 nm.

Nanocomposite films, in which nanoparticles with two different sizes, are embedded, and are formed for exploring size effect for immobilized photocatalytic nanoparticles. The photocatalytic activity comparison of these nanocomposite films under activation with 330 nm monochromatic light under the same condition is studied in Fig. 3.2.3. Smaller sized TiO_2 nanocomposite film has higher photocatalytic activity than the larger sized one. One reason for the increased photocatalytic activity with smaller size is the increased active surface area due to the increased surface to volume ratio. Another reason is the quantum confinement effect resulting from the smaller size.

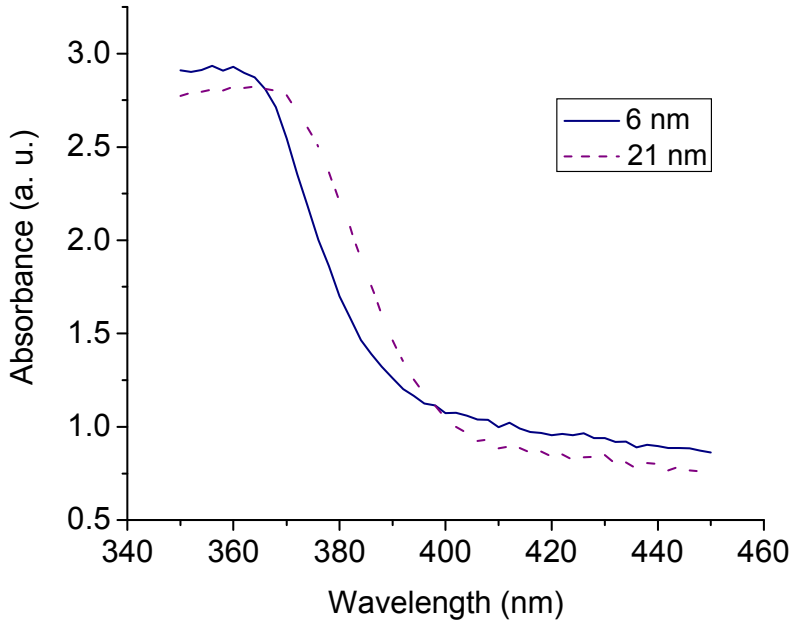

Figure 3.2.4 Absorbance spectra of the TiO_2 nanocomposite films with nanoparticle sizes of 6 nm and 21 nm in diameter.

Optical absorption spectra of 6 nm and 21 nm TiO_2 nanocomposite films are shown in Fig. 3.2.4. Shrinking the size from 21 nm to 6 nm results in an increase in the forbidden band due to the quantum confinement [15]. It is demonstrated in Fig. 3.2.4. Widening of the band gap leads to an increase in the energy of conduction band electrons and valence band holes. Better matching with the redox potentials of the adsorbates due to the shift in the conduction band minimum and the valence band maximum results in an increased activity in the reduction of the acceptor and in the oxidation of the donor [8, 33].

For the control group experiment in Fig. 3.2.5, we used acrylic sol-gel film without any photocatalyst inside. It is the host matrix we used in which nanoparticles are embedded for photocatalytic applications. Acrylic sol-gel film is irradiated with 330 nm monochromatic light with activation energies from 9.5 J/cm^2 to 47.5 J/cm^2. A slight bleaching is observed for methylene blue, which is due to direct photolysis. It has also a positive effect for the degradation of the contaminant which is desirable. The contribution coming from direct photolysis

is very small when compared with the photocatalytic recovery of the catalyst nanocomposite film. So the main contribution of degradation of the contaminants in the presence of TiO_2 nanoparticles comes from the photocatalytic activity [15].

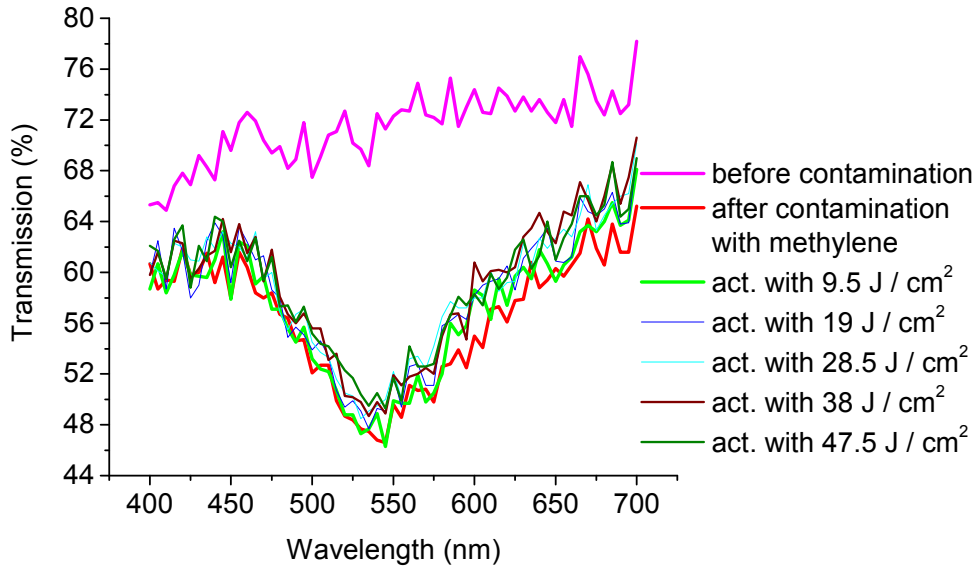

Figure 3.2.5 Optical transmission spectra of acrylic film for control experiment; contaminated with methylene blue and activated under UV light at 330 nm with excitation density ranging from 9.5 J/cm^2 up to 47.5 J/cm^2.

3.3 Effect of recontamination and reactivation

TiO_2 (6 nm) nanocomposite film that is activated at 330 nm at optical activation ranging from 10.8 J/cm^2 up to 54 J/cm^2 is used for recontamination and reactivation purposes. After the first activation with optical excitation density of 54 J/cm^2, the optical recovery level was about 68% (Fig. 3.3.1). The same sample is recontaminated and exposed to UV irradiation of 330 nm for a shorter time than the previous activation (activated with nearly half of the previous activation energy/unit area) [15].

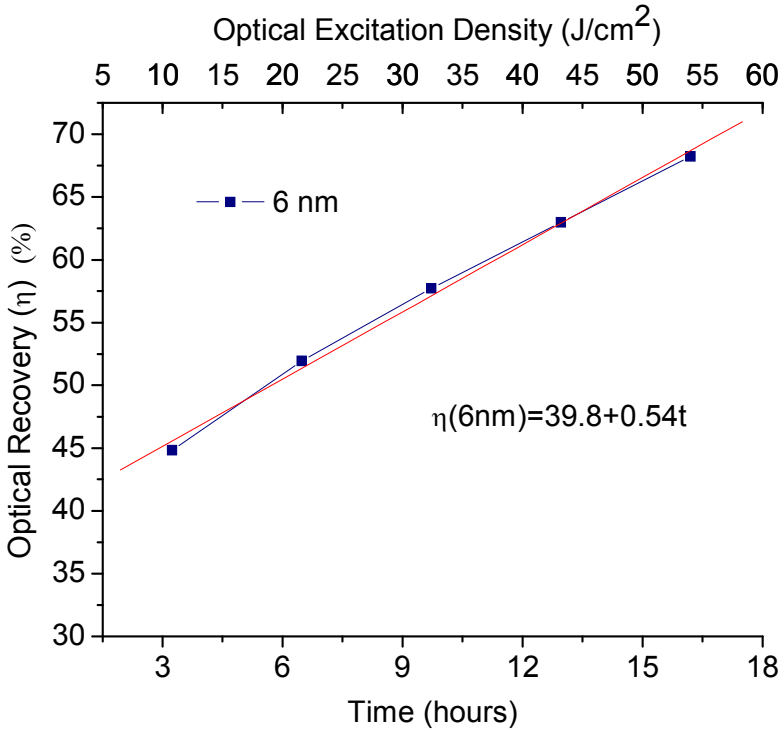

Figure 3.3.1 Optical recovery levels of TiO_2 nanocomposite film with nanoparticle diameter of 6 nm after it is photocatalytically self-cleaned from methylene blue.

The reactivation following the recontamination is performed with optical excitation density of 32 J/cm^2. The optical recovery level obtained at the end of UV irradiation at 330 nm is about 85% with a higher increase than the first activation process [15]. The optical recovery achieved for the first experiment after the same amount of activation (32 J/cm^2) was ~ 58% in Fig. 3.3.1. The reason for a better activity for the reactivation after recontamination is due to the surface structural change of TiO_2 crystal lattice reacting with water molecules [39, 52, 53].

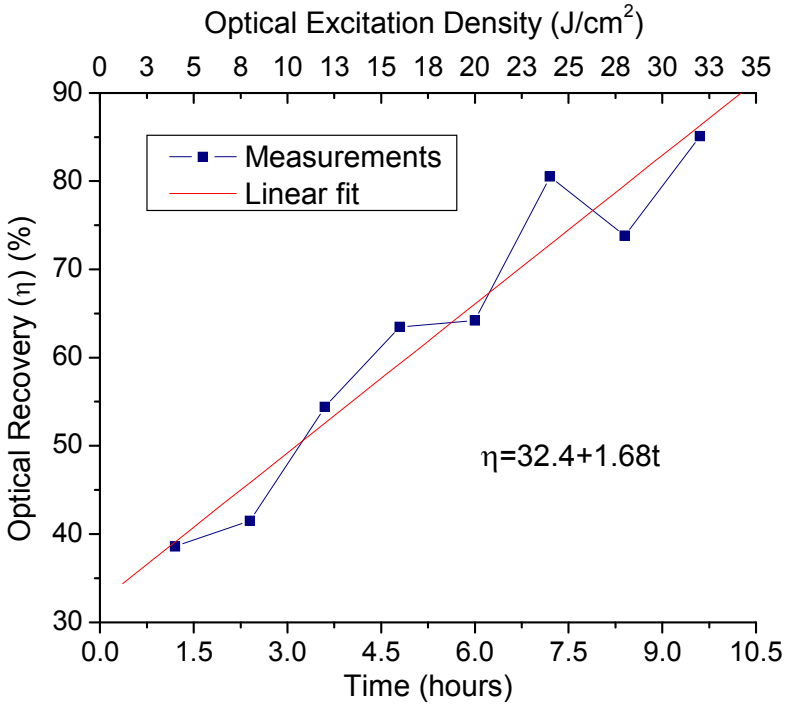

Figure 3.3.2 Optical recovery levels of TiO_2 nanocomposite film with nanoparticles diameter of 6 nm after it is photocatalytically self-cleaned from methylene blue, contaminated again, and photocatalytically reactivated at the same wavelength.

3.4 Activation Wavelength

The optical activation wavelength has an important effect on the photocatalytic recovery levels. The band gap energy of semiconductor metal-oxide limits the photocatalytic activity at higher wavelengths with photon energies smaller than the forbidden gap. The spectral photocatalytic response of TiO_2 and ZnO nanocomposite films are investigated in sections 3.4.1 and 3.5, for defining the optimal activation wavelength ranges. In the literature, though the effect of activation wavelength on photocatalytic activity is mentioned [54]. However there is no complete study of photocatalytic activity for different excitation wavelengths ranging from UV to visible.

3.4.1 Optical spectral response of ZnO

The nanocomposite film is formed through chemical integration of ZnO nanoparticles into three dimensional poly(vinylacetate)/ poly(methylmethacrylate) host resin. ZnO nanoparticles are 100 nm in diameter. We contaminate our samples with the standard methylene blue by spray coating and optically activate them under UV illumination with known activation wavelength and intensity for the certain periods of time. After analyzing the experimental data, the resulting photocatalytic recovery levels are plotted as a function of the excitation wavelength. Here every data point corresponds to an experiment of ZnO nanocomposite films conducted under exactly the same conditions.

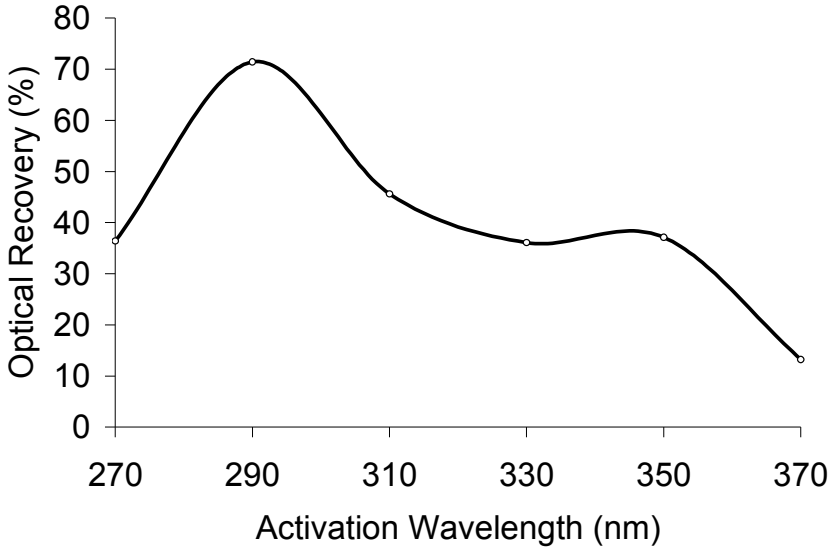

Figure 3.4.1.1 Optical recovery levels achieved at the end of 8 hours activation (7.3 J/cm^2) at different wavelengths ranging from 270 nm to 370 nm.

The optical recovery is the largest at an excitation of 290 nm. The increased photocatalytic recovery at activation wavelengths below 370 nm is expected.

The photocatalytic activity decreases at excitation wavelengths below 290 nm. One reason for this drop can be the decreased adsorptive capacity of the catalyst resulting from the increased temperature due to higher energy photon recombination [26].

3.5 Comparative study of TiO_2 and ZnO nanocomposite films

TiO_2 nanoparticles and ZnO nanoparticles, which are 6 nm and 150 nm in diameters, respectively, are immobilized through full chemical integration into sol-gel matrix. Nanocomposite sol-gel is applied on acetate film through spray coating method. The mass ratio of nanoparticles embedded into the host sol-gel is 6.0% for TiO_2 and 9.5% for ZnO. The resulting films are 10 μm in thickness.

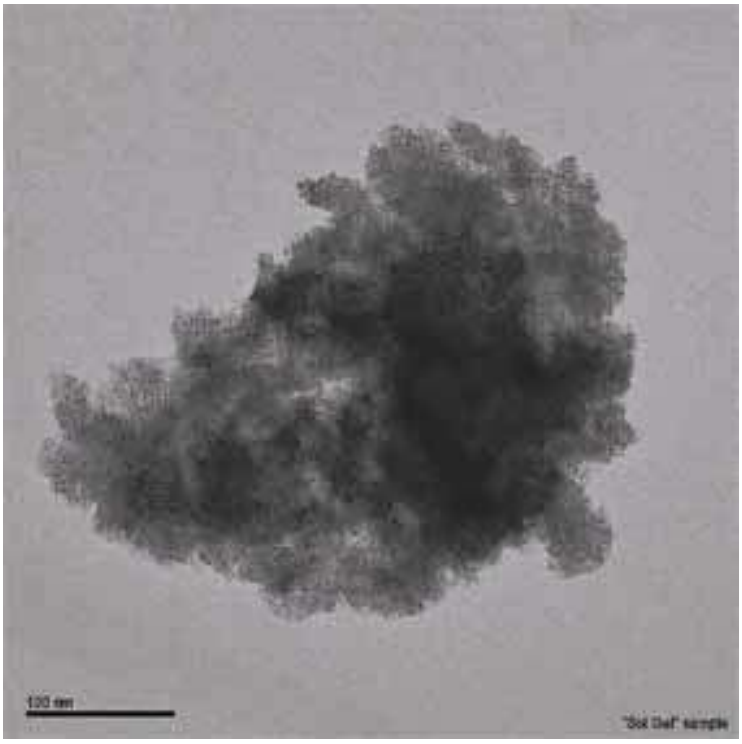

Figure 3.5.1 TEM image of the prepared sol-gel.

During the sol-gel synthesis, two types of silicon alkoxides were used to obtain the hybrid organic-inorganic material that leads to the formation of a three dimensional silica network. The solvent plays an important role to control the formation and properties of silica gels. Thus, to achieve an appropriate host resin, we used ethyl alcohol and iso-propyl alcohol. Hydrolysis and condensation rates of silicon alkoxides were further enhanced by HCl (0.1 N) catalysis. Reaction initiation temperature was 50ºC. Nanoparticle dispersion integrated into the resulting solgel was applied on acetate film through spray coating method. As a result of the chemical integration, we obtained nanocomposite materials with their nanoparticles dispersed more uniformly than mere blending. Here we used TiO_2 nanoparticles of 6 nm in size and ZnO nanoparticles of 150 nm in size, with the mass ratio of the incorporated nanoparticles to the host solgel of 6.0% for TiO_2 and of 9.5% for ZnO in thin films of about 10 μm in thickness [16].

Optical recovery levels are obtained for each sample activated at a monochromatic wavelength as a function of the incident total optical excitation density increased from 1.8 J/cm^2 to 7.3 J/cm^2. In Fig. 3.5.2, smaller TiO_2 nanoparticles have a general behavior of higher photocatalytic activity than larger size ZnO nanoparticles although it has lower concentration than ZnO. Also ZnO is reported to have higher quantum efficiency in the literature [55]. Thus we demonstrate that nanoparticle quantum size effect and the increased surface to volume ratio with larger active surface area of the photocatalyst have an important effect on the activity of the photocatalytic film in addition to the type of the photocatalyst.

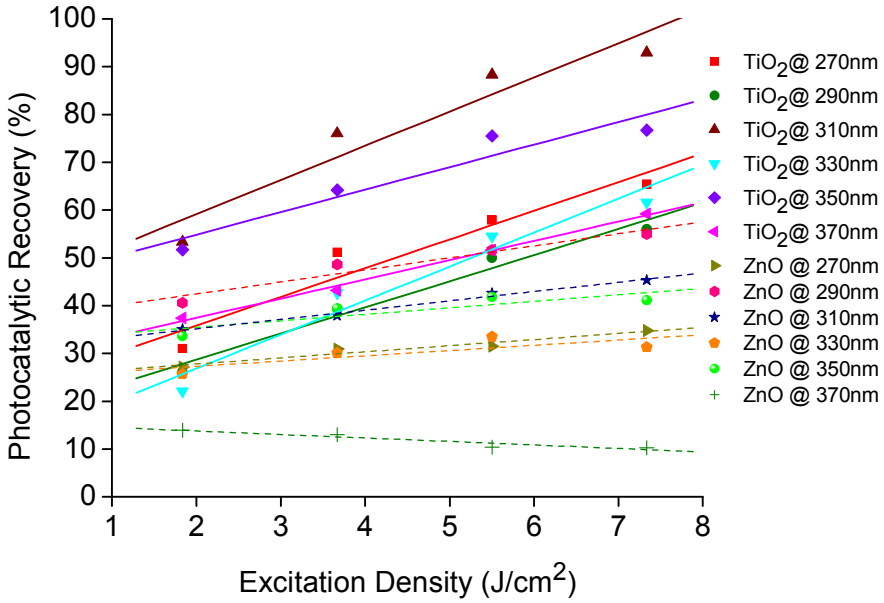

Figure 3.5.2 Relative spectral photocatalyic recovery levels of TiO_2 and ZnO nanocomposite films at monochromatic activation wavelengths (270-370 nm) as a function of incident total optical excitation density (incident optical intensity *x* time).

In this implementation, TiO_2 has its highest photocatalytic activity when excited at wavelength of 310 nm. ZnO has its optimum photocatalytic activity when excited at 290 nm, which is the same result we obtained using a different host resin, poly(vinylacetate)/ poly(methylmethacrylate in another experiment set. The highest optical recovery level of TiO_2 is 93% when activated with 310 nm and of ZnO is 55% when activated with 290 nm. This result indicates that combinations of TiO_2 and ZnO nanoparticles integrated in the same resin can be used to tune the optimal activation wavelength [16, 48].

Activation Wavelength	270 nm	290 nm	310 nm	330 nm	350 nm	370 nm
TiO_2	6.00	5.47	7.15	7.10	4.70	4.02
ZnO	1.28	2.52	1.94	1.10	1.36	-0.73

Table 3.5.1 Relative differential photocatalytic activities of TiO_2 and ZnO nanocomposite films ($1/J/cm^2$).

The slopes of the linear fits to the photocatalytic recovery curves are given in Table 3.5.1. The differential photocatalytic activities at different activation wavelengths for both TiO_2 and ZnO nanocomposite films are obtained as a figure of merit to represent the incremental photocatalytic activity per unit optical excitation density. TiO_2 has higher differential activity than ZnO, in addition to its higher photocatalytic activities at all activation wavelengths. Also a good correlation is observed between the differential photocatalytic activity and the photocatalytic activity, both of which have the highest values at the optimum excitation wavelength for both TiO_2 (7.15×10^{-4}at 310 nm) and for ZnO (2.52×10^{-4} at 290 nm). The photocatalytic recovery curves require larger slopes to reach high levels of recovery within a finite period of optical activation at a constant optical intensity [16].

3.6 Combination of TiO_2-ZnO nanoparticles chemically integrated into acrylic for enhanced

photocatalytic activity in the near-UV and the visible

Since photocatalytically active semiconductor metal oxides are wide bandgap semiconductors, they cannot be activated under sunlight. They show high photocatalytic activities under ultraviolet irradiation below 380 nm, which have higher energies than the forbidden band of those catalysts. The part of spectrum that these nanoparticles can be photocatalytically activated is very important especially when these immobilized forms are used for the decontamination of large outdoor areas under sunlight.

TiO_2 nanoparticles (6 nm in diameter) and ZnO nanoparticles (150 nm in diameter) are chemically integrated into the same resin to enhance the photocatalytic activity in the near-UV and the visible spectral ranges that make higher content of the sunlight. A hybrid nanocomposite material is formed through immobilization of the same amount of TiO_2 (8.5% mass ratio) and ZnO (8.5% mass ratio) nanoparticles in the same acrylic sol-gel resin with a better dispersion than simple blending. Only TiO_2 and only ZnO nanocomposite films are formed with the same total metal-oxide concentration of 17% for comparison purposes.

In the literature, there is a significant amount of research work on the photocatalytic activities of immobilized TiO_2 and ZnO nanoparticles seperately in thin film [8, 12, 56, and 57]. The combination of TiO_2 and ZnO nanoparticles integrated into a single film, however, remains to be unexplored.

The host acrylic sol-gel resin provides a homogenous distribution of the metal-oxide nanoparticles inside the three dimensional matrix with a very low number of aggregates. Despite the decreased active surface area due to the immobilization, semiconductors have very high photocatalytic activities. Hybrid organic-inorganic material formation via sol-gel route prevents the

photocatalytic degradation of the host resin with these highly active nanoparticles. The optical recovery levels measured during the activation of nanocomposite films only come from the degradation of the contaminant methylene blue.

In the literature, some research work is available for the enhancement of the photocatalytic activity by incorporating various semiconductors [18, 40, 41-43, 58]. These semiconductors are incorporated in the interlayer of the layered compounds for nanocomposite film fabrication. Higher photocatalytic activities compared to the unsupported photocatalysts are reported [18]. Besides the difference of their method and the limited applicability when compared to ours, no optical spectral study is conducted to find out the wavelength range where the enhancement occurs. The nanocomposite films formed with various techniques in the literature are mostly activated with direct sunlight [18], with a UV lamp consisting of only UV content [41, 42] or at a single fixed activation wavelength [40]. Enhancement in deeper UV wavelengths has no significance if we consider photocatalytic decontamination under sunlight. With the use of chemically integrated TiO_2-ZnO combined nanocomposite film, our study contributes to the literature with the discovery and demonstration of enhancement in the photocatalytic recovery achieved under irradiation with the near-UV and the visible light.

3.6.1 Activations in the ultraviolet and the visible

Three sets of nanocomposite films are formed by spray coating method, each with a 10 μm thickness:

1) Combination of TiO_2-ZnO nanoparticles (8.5% of TiO_2 and 8.5% of ZnO mass ratios [17% of total metal-oxide] in the dispersion) in acrylic sol-gel film,

2) Only TiO_2 nanoparticles (17% mass ratio in dispersion) in acrylic sol-gel film,

3) Only ZnO nanoparticles (17% mass ratio in dispersion) in acrylic sol-gel film.

Also, acrylic sol-gel film on acetate without any metal-oxides is formed for control group experiments.

Methylene blue is used as the standard contaminant. Contamination is carried out through drop casting and waiting for 30 minutes for every sample to achieve the same amount of contamination. A Xenon light source and a monochromator (Digikröm CM110) are used for the activation of contaminated samples at 16 specific wavelengths from 310 nm to 469 nm. The total number of incident activation photons per unit area is kept constant at

$$[\text{activation power x time}] / [\text{spot size x photon energy}] = 10^{22}\text{m}^{-2}$$

We choose the exposure times in minutes (a few to tens of minutes) and activation powers were tens to hundreds of microwatts to obtain the photocatalytic recovery levels for all three kinds of nanocomposite films on the same recovery scale from zero to hundred percent for better comparison. We use the same contamination level of around 20% for all samples. These chosen parameters are important for photocatalytic activity comparison of those three nanocomposite films activated at different activation wavelengths. If a smaller amount of contamination is chosen, all the methylene blue can be degraded by TiO_2 film at 310 nm and TiO_2 cannot find contaminant to further degrade for the continuing activation period. This will make the comparative study impossible. Also if we choose longer activation time, the same problem can occur.

An experiment set is shown in Fig. 3.6.1.1. Nanocomposite films and the control group film are activated at 330 nm after they are contaminated with methylene blue. The decrease in the optical transmission of film is observed after it is contaminated. Optical transmission curve recovers its optical level during the optical activation at 330 nm due to the degradation of methylene blue.

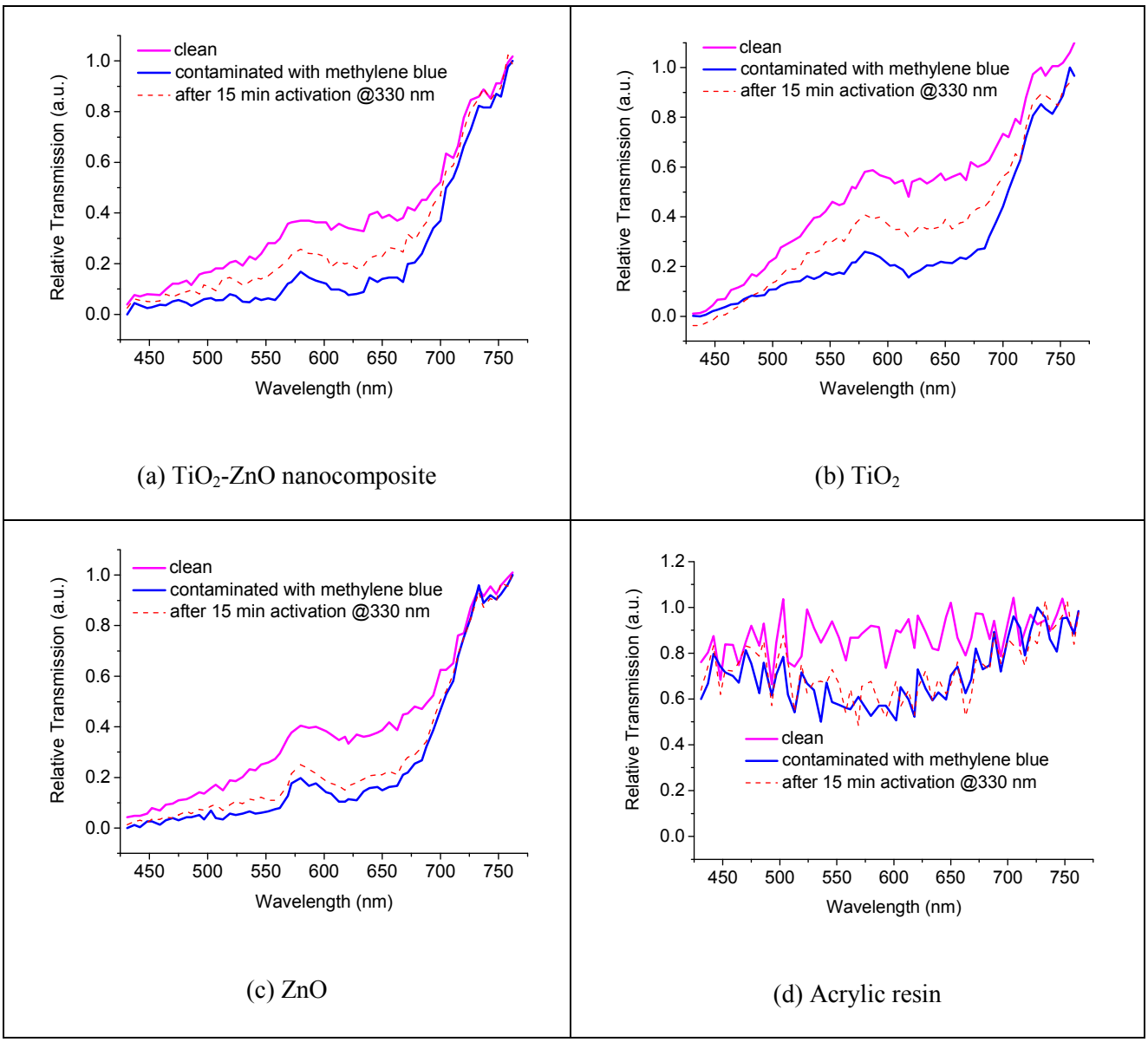

Figure 3.6.1.1 Optical transmission spectra of the films consisting of (a) TiO_2-ZnO combined nanocomposite, (b) only TiO_2, and (c) only ZnO nanocomposites before and after they are contaminated with methylene blue, and after they are photocatalytically activated at 330 nm keeping the total number of incident activation photons per unit area ([activation power x time] / [spot size x photon energy] constant at 10^{22} m^{-2} along with (d) the host resin without any nanoparticles as the control group.

TiO_2 nanocomposite film is the most active when activated at 330 nm. In the literature, ZnO is reported to be a good alternative for TiO_2 when it is used in photocatalysis [55]. However smaller sized TiO_2 is always a better photocatalyst than the larger sized ZnO nanocomposite film. TiO_2-ZnO combination's photocatalytic activity at 330 nm is between the TiO_2 and ZnO nanocomposite films with a nearer level to TiO_2 nanocomposite film. The photocatalytic recovery levels at 330 nm activation are 59% for TiO_2 nanocomposite, 20% for ZnO nanocomposite and 43% for TiO_2-ZnO nanocomposite films. Optical recovery level for the control group is insignificant (2.2%) as we expected.

Another experiment set is conducted at activation wavelength of 403 nm where we do not expect significant photocatalytic activities with the use of only TiO_2 and only ZnO nanocomposite films. Fig. 3.6.1.2 demonstrates the photocatalytic activity in the visible with the use TiO_2- ZnO combined nanocomposite.

The photocatalytic recovery levels at 403 nm activation are 13% for TiO_2 nanocomposite, 1% for ZnO nanocomposite and 24% for TiO_2-ZnO nanocomposite films. The control group has recovery level of 4.9%. Photocatalytic synergy effect at excitation in the visible is observed with the use of TiO_2-ZnO combination immobilized in a single film.

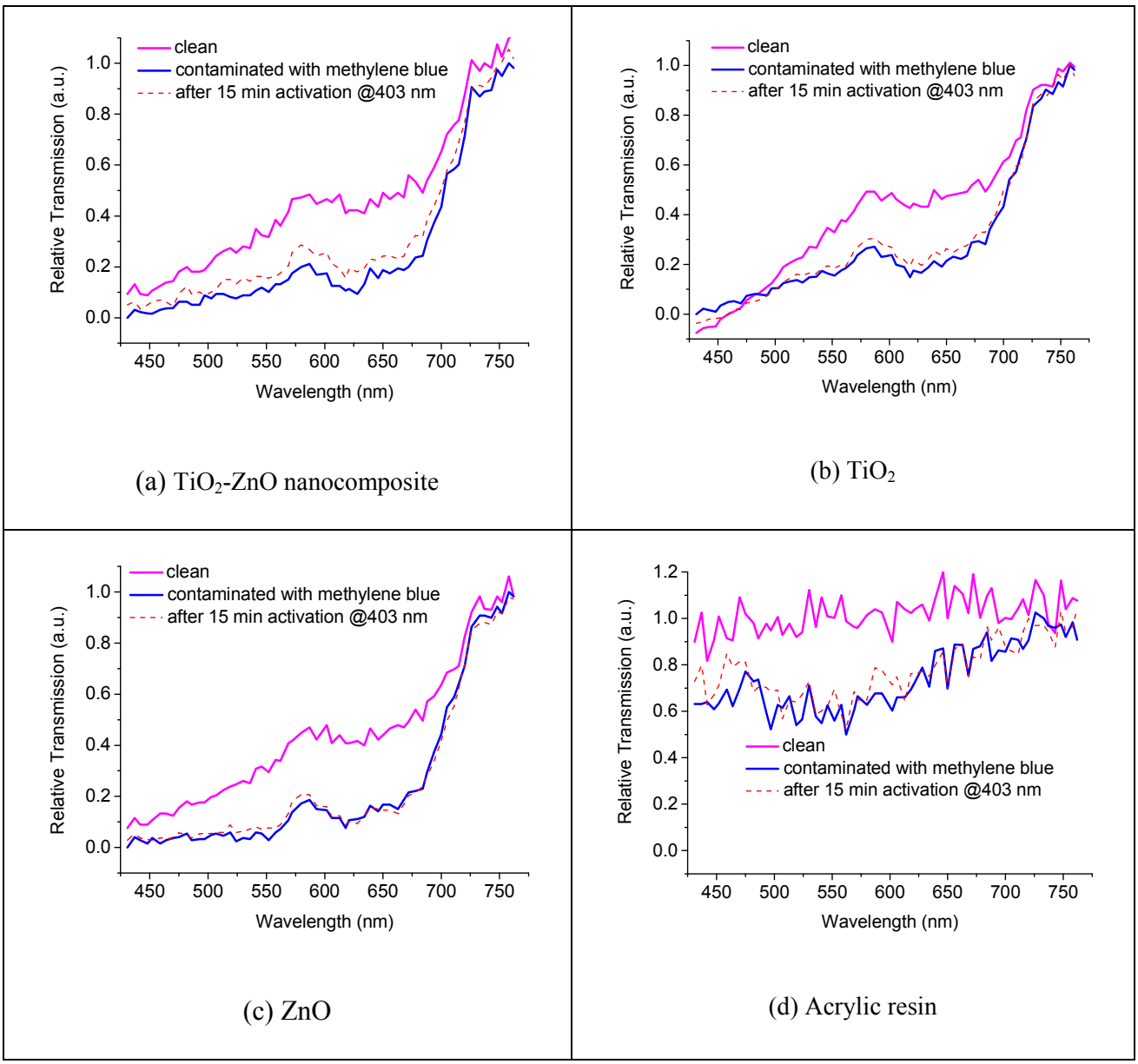

Figure 3.6.1.2 Optical transmission spectra of the films consisting of (a) TiO_2-ZnO combined nanocomposite, (b) only TiO_2, and (c) only ZnO nanocomposites before and after they are contaminated with methylene blue, and after they are photocatalytically activated at 403 nm keeping the total number of incident activation photons per unit area ([activation power x time] / [spot size x photon energy] constant at 10^{22} m^{-2} along with (d) the host resin without any nanoparticles as the control group.

64 photocatalytic experiments at 16 different monochromatic activation wavelengths between 310 nm and 469 nm are conducted under the same conditions for all three types of nanocomposite films and the control group

films. Here we put the experimental results of these 32 photocatalytic experiments at 8 separate activation wavelengths (310 nm, 330 nm, 350 nm, 370 nm, 393 nm, 416 nm, 437 nm, and 458 nm) in Figures 3.6.1.3-3.6.1.10.

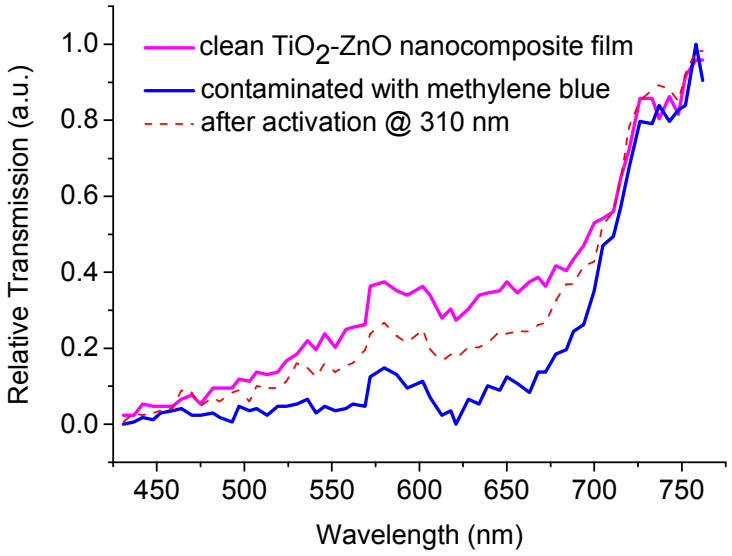

(a)

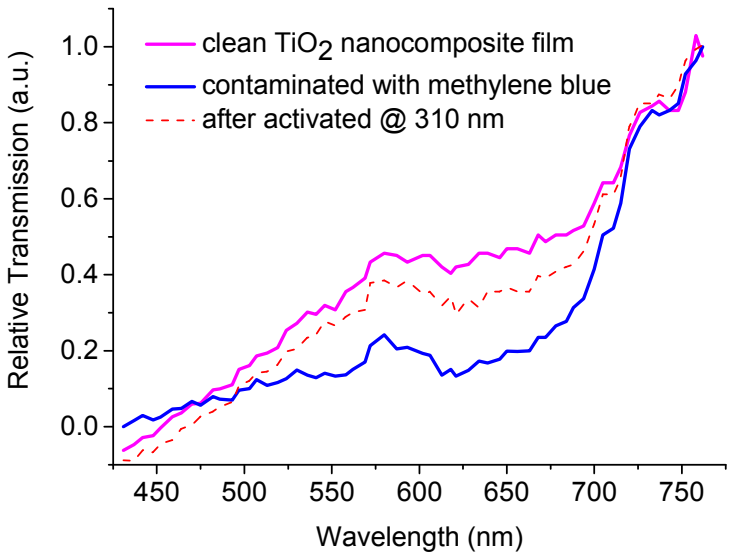

(b)

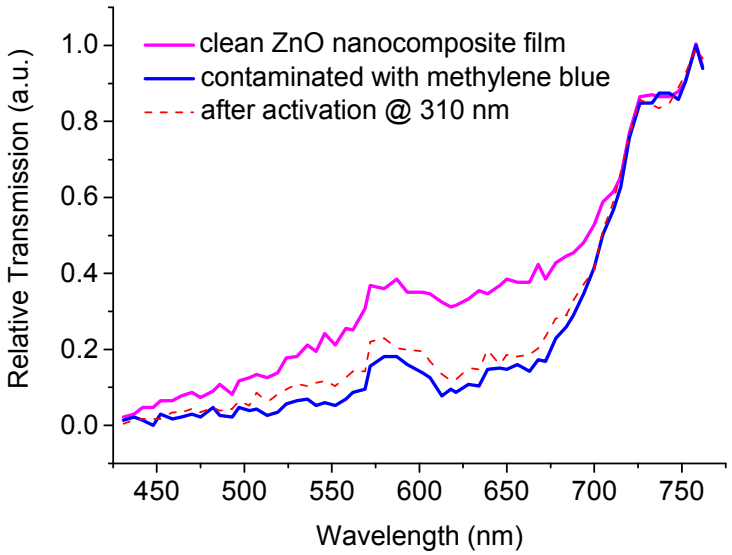

(c)

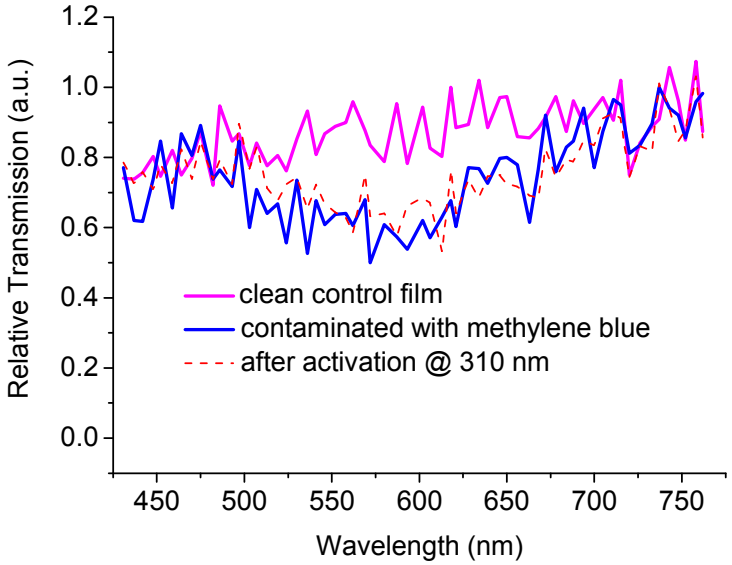

(d)

Figure 3.6.1.3 Optical transmission spectra of the films consisting of (a) TiO_2-ZnO combined nanocomposite, (b) only TiO_2, and (c) only ZnO nanocomposites before and after they are contaminated with methylene blue, and after they are photocatalytically activated at 310 nm keeping the total number of incident activation photons per unit area ([activation power x time] / [spot size x photon energy] constant at 10^{22} m^{-2} along with (d) the host resin without any nanoparticles as the control group.

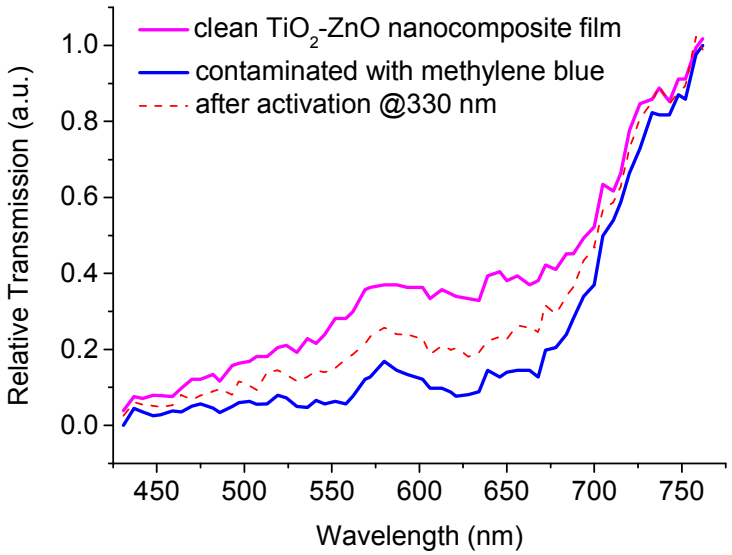
clean TiO2-ZnO nanocomposite film
contaminated with methylene blue
after activation @330 nm
Relative Transmission (a.u.)
1.0
0.8
0.6
0.4
0.2
0.0
450
500
550
600
650
700
750
Wavelength (nm)

(a)

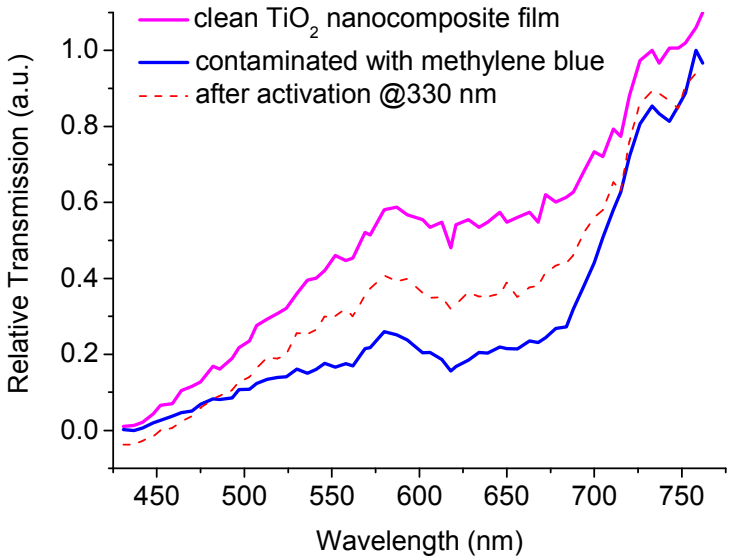
clean TiO2 nanocomposite film
contaminated with methylene blue
after activation @330 nm
Relative Transmission (a.u.)
1.0
0.8
0.6
0.4
0.2
0.0
450
500
550
600
650
700
750
Wavelength (nm)

(b)

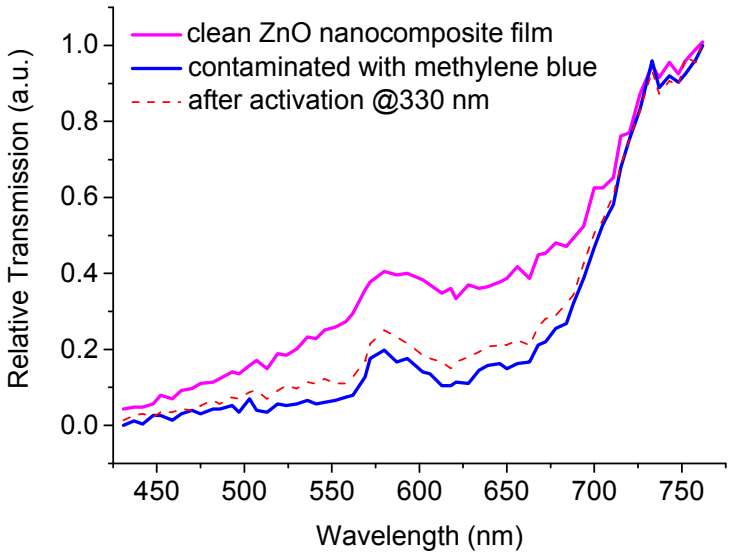

(c)

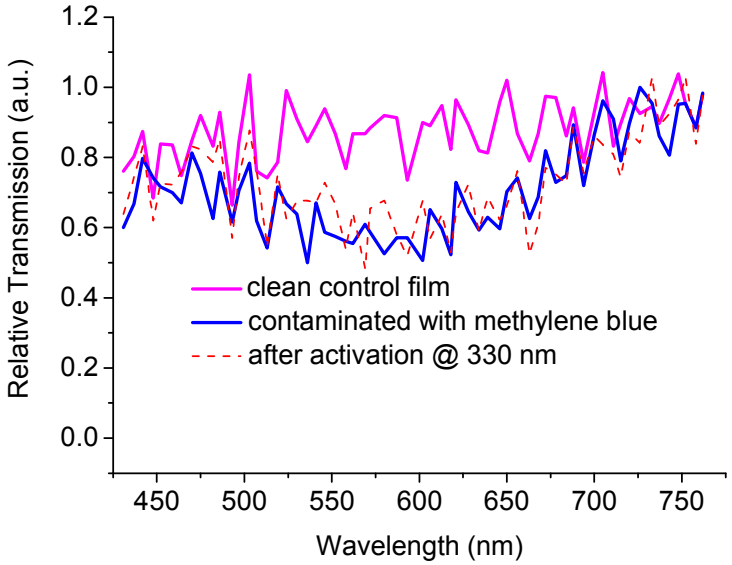

(d)

Figure 3.6.1.4 Optical transmission spectra of the films consisting of (a) TiO_2-ZnO combined nanocomposite, (b) only TiO_2, and (c) only ZnO nanocomposites before and after they are contaminated with methylene blue, and after they are photocatalytically activated at 330 nm keeping the total number of incident activation photons per unit area ([activation power x time] / [spot size x photon energy] constant at 10^{22} m^{-2} along with (d) the host resin without any nanoparticles as the control group.

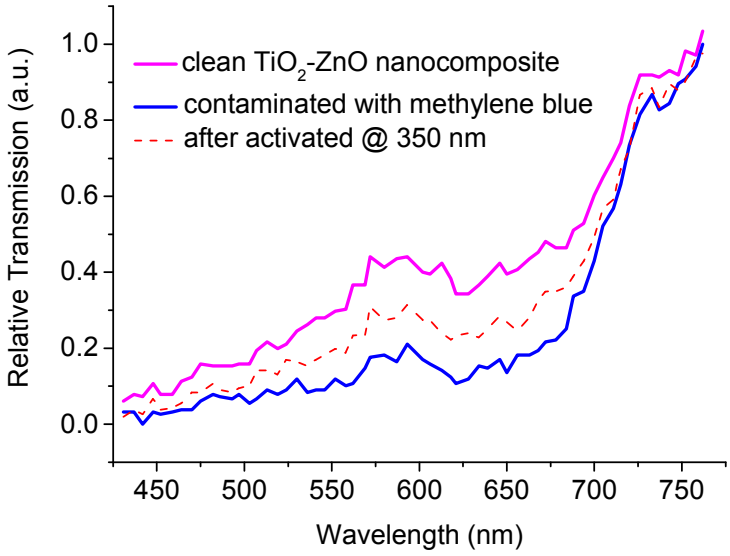
clean TiO2-ZnO nanocomposite
contaminated with methylene blue
after activated @ 350 nm
Relative Transmission (a.u.)
Wavelength (nm)
1.0
0.8
0.6
0.4
0.2
0.0
450
500
550
600
650
700
750

(a)

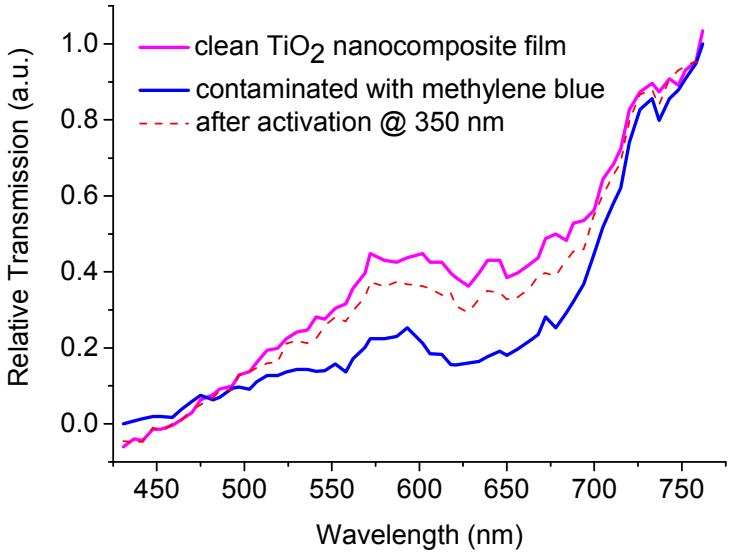
clean TiO2 nanocomposite film
contaminated with methylene blue
after activation @ 350 nm
Relative Transmission (a.u.)
Wavelength (nm)
1.0
0.8
0.6
0.4
0.2
0.0
450
500
550
600
650
700
750

(b)

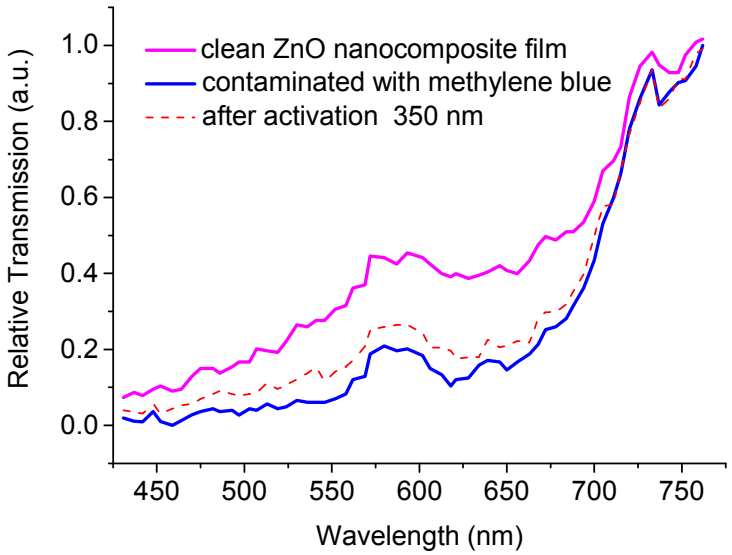

(c)

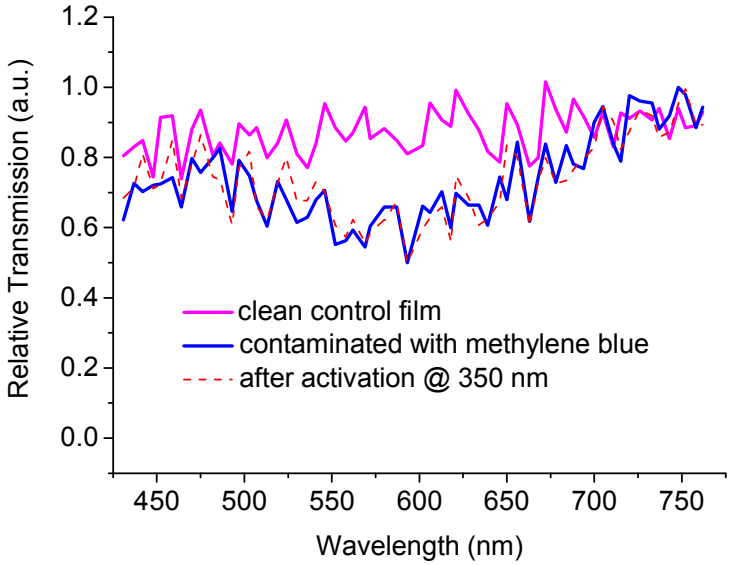

(d)

Figure 3.6.1.5 Optical transmission spectra of the films consisting of (a) TiO_2-ZnO combined nanocomposite, (b) only TiO_2, and (c) only ZnO nanocomposites before and after they are contaminated with methylene blue, and after they are photocatalytically activated at 350 nm keeping the total number of incident activation photons per unit area ([activation power x time] / [spot size x photon energy] constant at 10^{22} m^{-2} along with (d) the host resin without any nanoparticles as the control group.

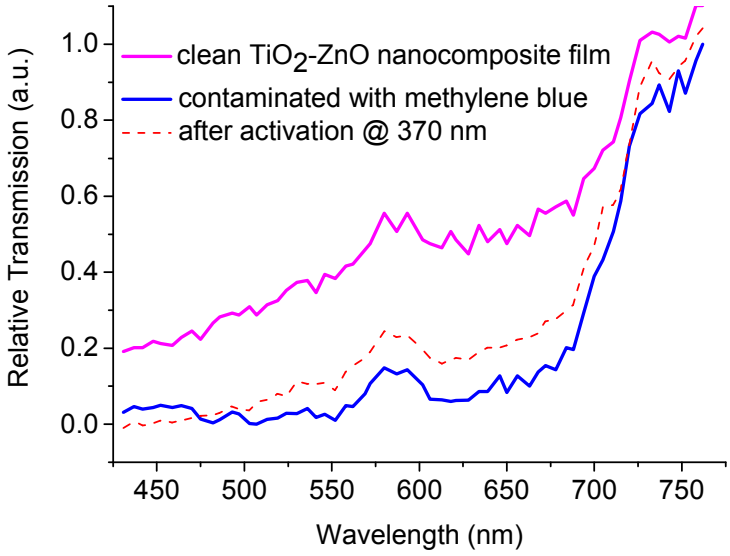
clean TiO2-ZnO nanocomposite film
contaminated with methylene blue
after activation @ 370 nm
Relative Transmission (a.u.)
Wavelength (nm)
1.0
0.8
0.6
0.4
0.2
0.0
450
500
550
600
650
700
750

(a)

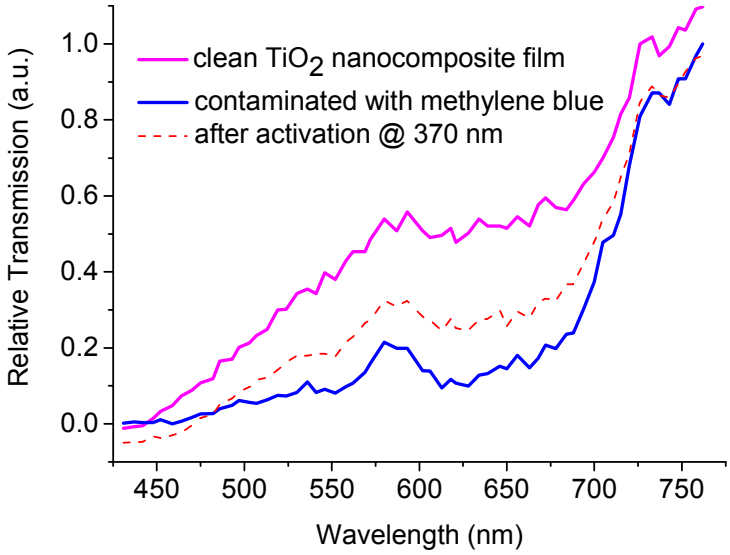
clean TiO2 nanocomposite film
contaminated with methylene blue
after activation @ 370 nm
Relative Transmission (a.u.)
Wavelength (nm)
1.0
0.8
0.6
0.4
0.2
0.0
450
500
550
600
650
700
750

(b)

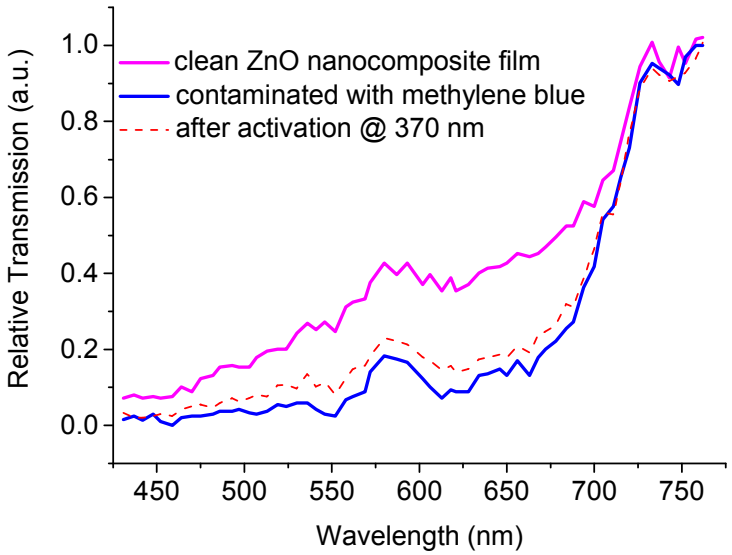

(c)

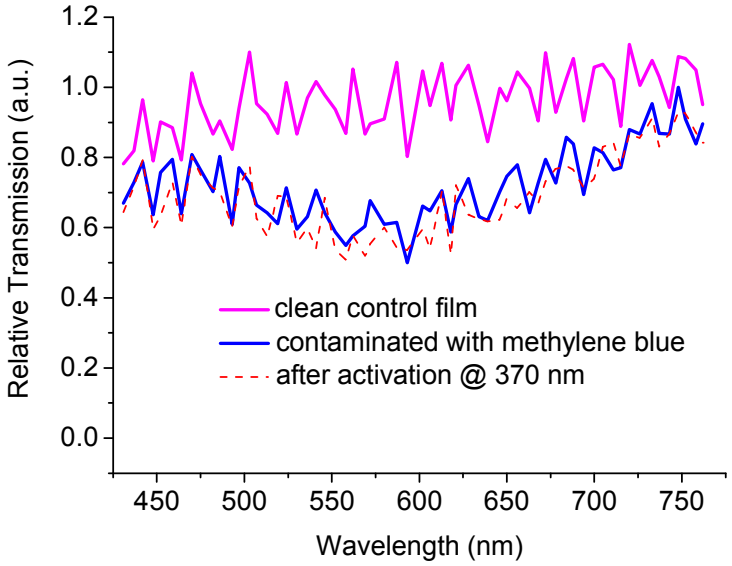

(d)

Figure 3.6.1.6 Optical transmission spectra of the films consisting of (a) TiO_2-ZnO combined nanocomposite, (b) only TiO_2, and (c) only ZnO nanocomposites before and after they are contaminated with methylene blue, and after they are photocatalytically activated at 370 nm keeping the total number of incident activation photons per unit area ([activation power x time] / [spot size x photon energy] constant at 10^{22} m^{-2} along with (d) the host resin without any nanoparticles as the control group.

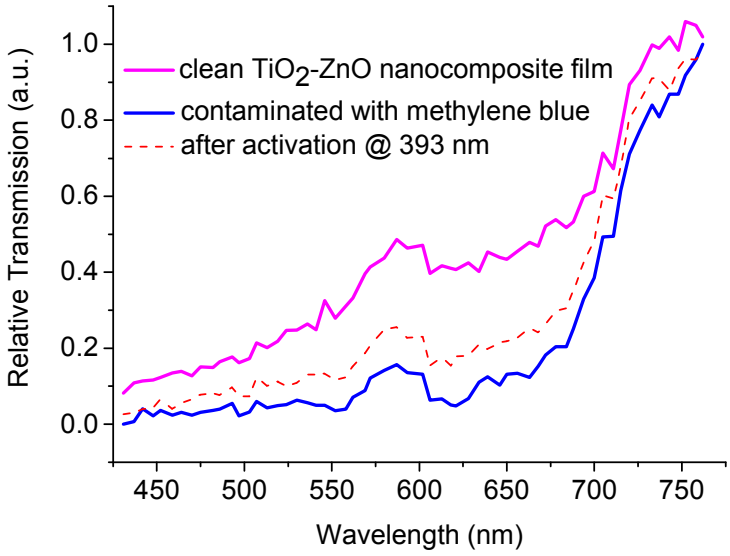
clean TiO2-ZnO nanocomposite film
contaminated with methylene blue
after activation @ 393 nm
Relative Transmission (a.u.)
Wavelength (nm)
1.0
0.8
0.6
0.4
0.2
0.0
450
500
550
600
650
700
750

(a)

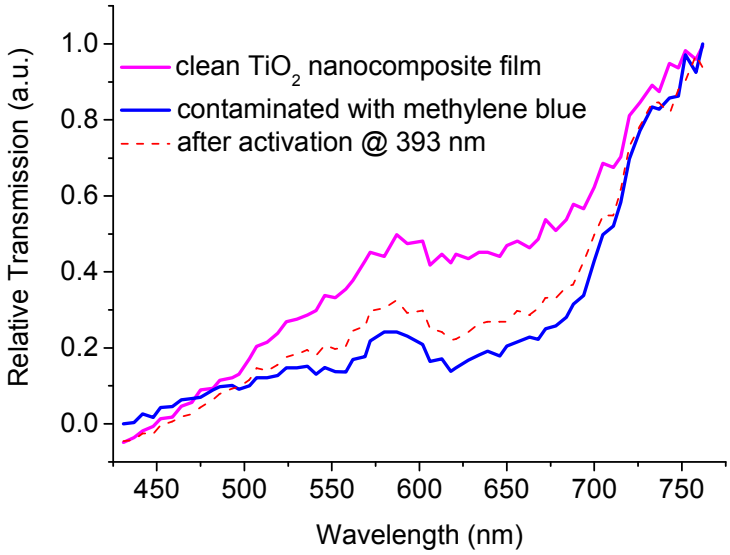
clean TiO2 nanocomposite film
contaminated with methylene blue
after activation @ 393 nm
Relative Transmission (a.u.)
Wavelength (nm)
1.0
0.8
0.6
0.4
0.2
0.0
450
500
550
600
650
700
750

(b)

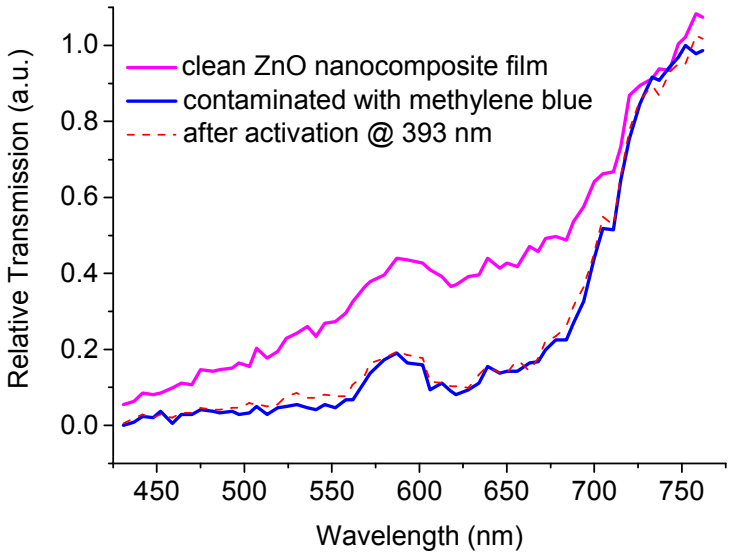

(c)

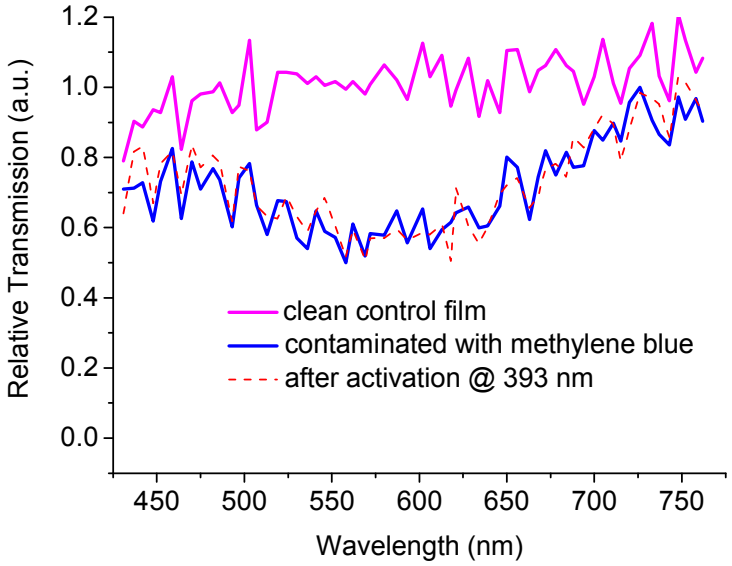

(d)

Figure 3.6.1.7 Optical transmission spectra of the films consisting of (a) TiO_2-ZnO combined nanocomposite, (b) only TiO_2, and (c) only ZnO nanocomposites before and after they are contaminated with methylene blue, and after they are photocatalytically activated at 393 nm keeping the total number of incident activation photons per unit area ([activation power x time] / [spot size x photon energy] constant at 10^{22} m^{-2} along with (d) the host resin without any nanoparticles as the control group.

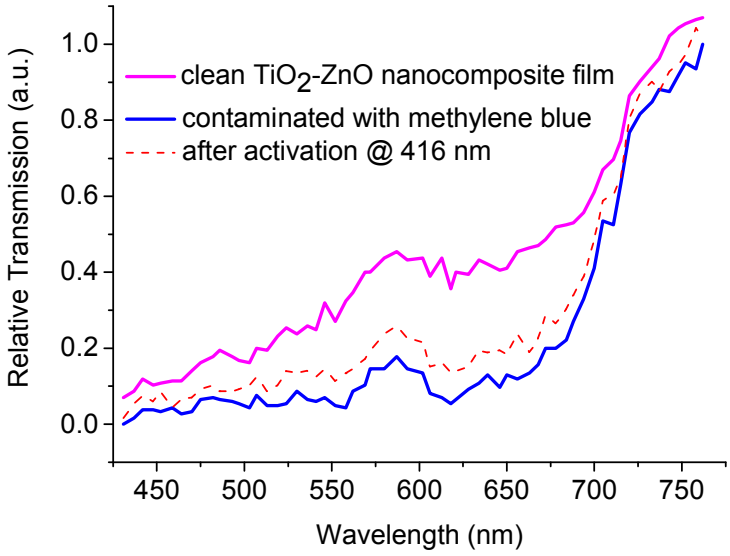
clean TiO2-ZnO nanocomposite film
contaminated with methylene blue
after activation @ 416 nm
Relative Transmission (a.u.)
Wavelength (nm)
1.0
0.8
0.6
0.4
0.2
0.0
450
500
550
600
650
700
750

(a)

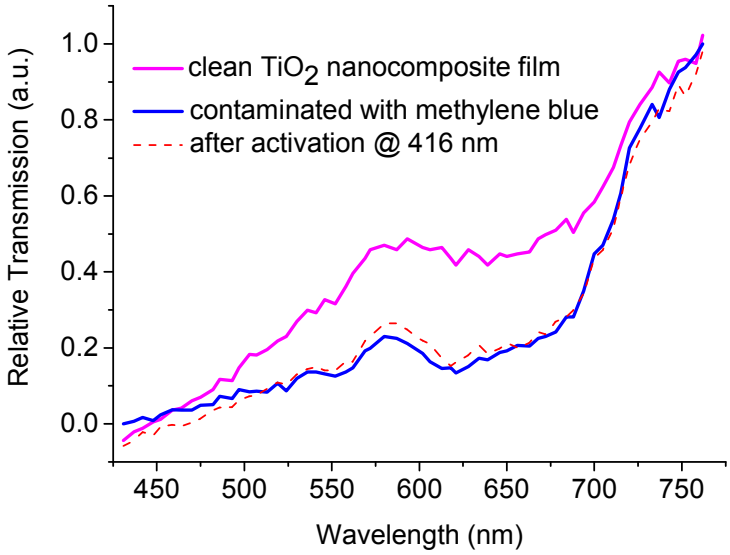
clean TiO2 nanocomposite film
contaminated with methylene blue
after activation @ 416 nm
Relative Transmission (a.u.)
Wavelength (nm)
1.0
0.8
0.6
0.4
0.2
0.0
450
500
550
600
650
700
750

(b)

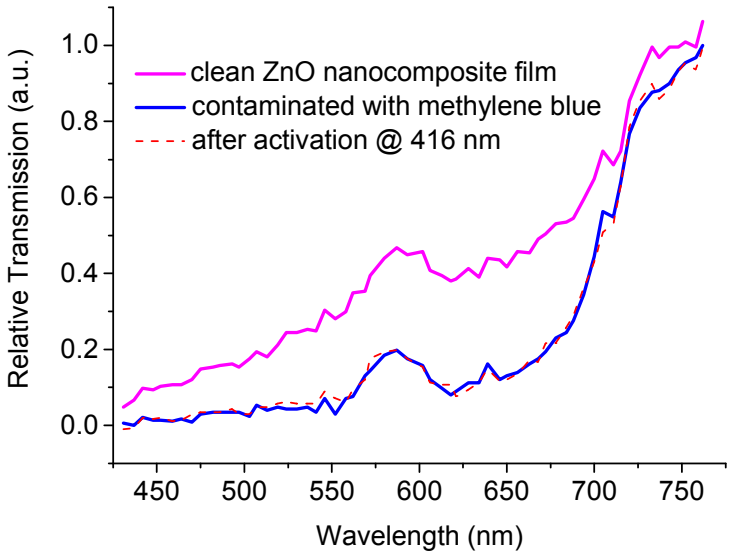

(c)

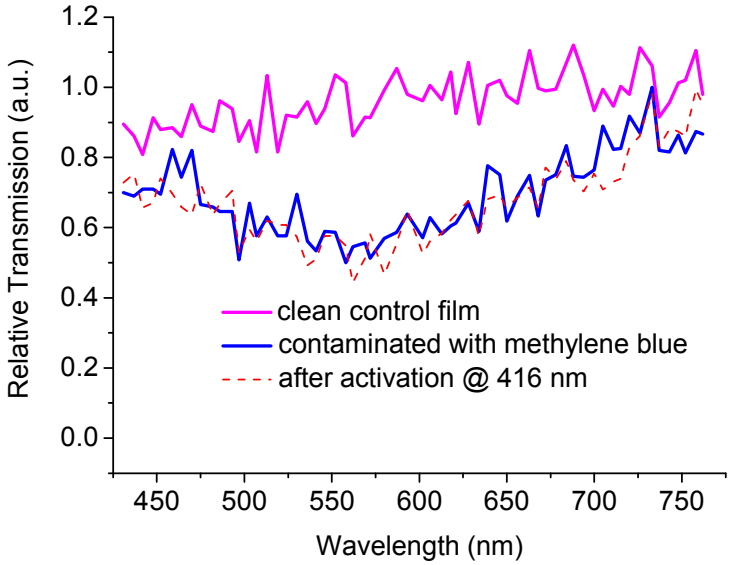

(d)

Figure 3.6.1.8 Optical transmission spectra of the films consisting of (a) TiO_2-ZnO combined nanocomposite, (b) only TiO_2, and (c) only ZnO nanocomposites before and after they are contaminated with methylene blue, and after they are photocatalytically activated at 416 nm keeping the total number of incident activation photons per unit area ([activation power x time] / [spot size x photon energy] constant at 10^{22} m^{-2} along with (d) the host resin without any nanoparticles as the control group.

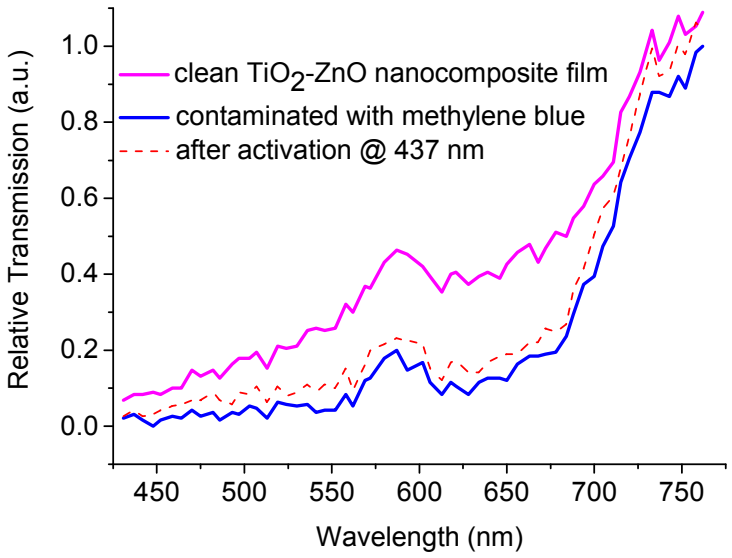
clean TiO2-ZnO nanocomposite film
contaminated with methylene blue
after activation @ 437 nm
Relative Transmission (a.u.)
Wavelength (nm)
1.0
0.8
0.6
0.4
0.2
0.0
450
500
550
600
650
700
750

(a)

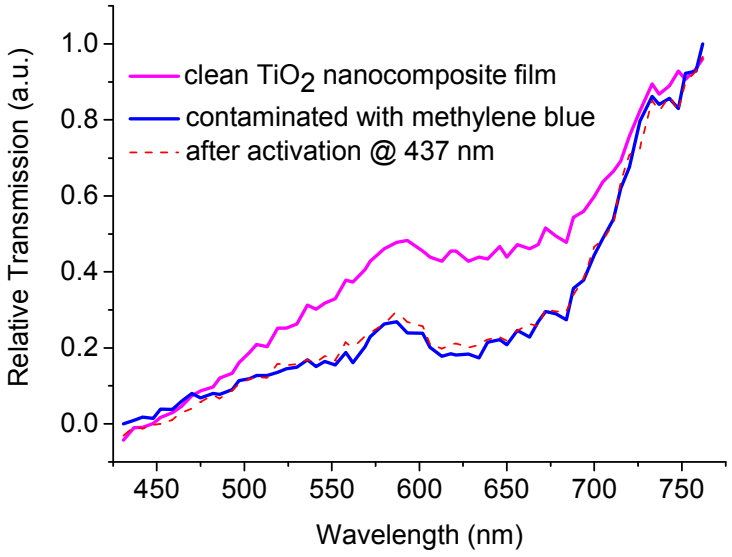
clean TiO2 nanocomposite film
contaminated with methylene blue
after activation @ 437 nm
Relative Transmission (a.u.)
Wavelength (nm)
1.0
0.8
0.6
0.4
0.2
0.0
450
500
550
600
650
700
750

(b)

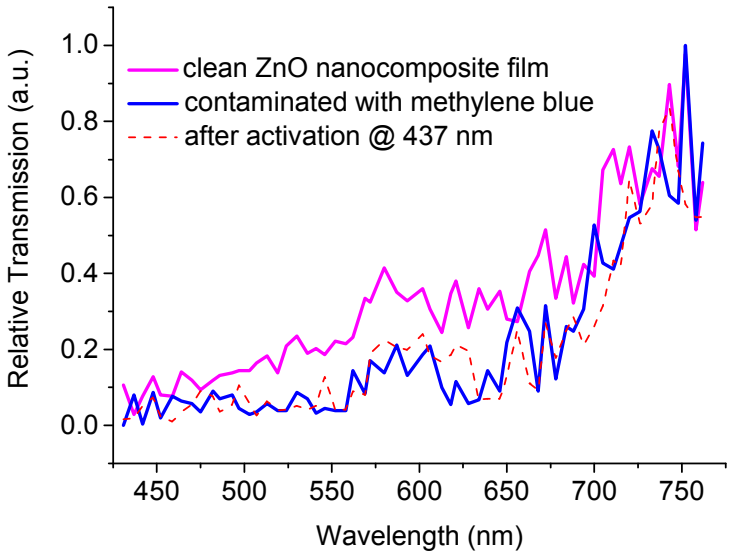

(c)

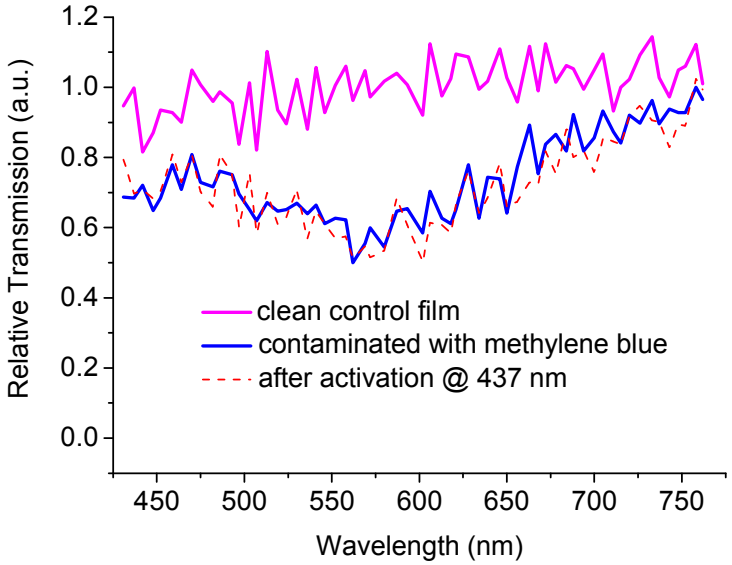

(d)

Figure 3.6.1.9 Optical transmission spectra of the films consisting of (a) TiO_2-ZnO combined nanocomposite, (b) only TiO_2, and (c) only ZnO nanocomposites before and after they are contaminated with methylene blue, and after they are photocatalytically activated at 437 nm keeping the total number of incident activation photons per unit area ([activation power x time] / [spot size x photon energy] constant at 10^{22} m^{-2} along with (d) the host resin without any nanoparticles as the control group.

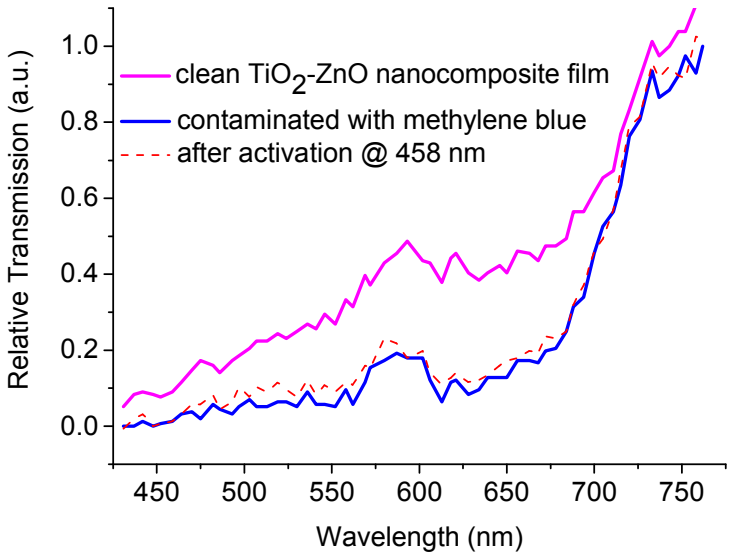
clean TiO2-ZnO nanocomposite film
contaminated with methylene blue
after activation @ 458 nm
Relative Transmission (a.u.)
Wavelength (nm)
0.0
0.2
0.4
0.6
0.8
1.0
450
500
550
600
650
700
750

(a)

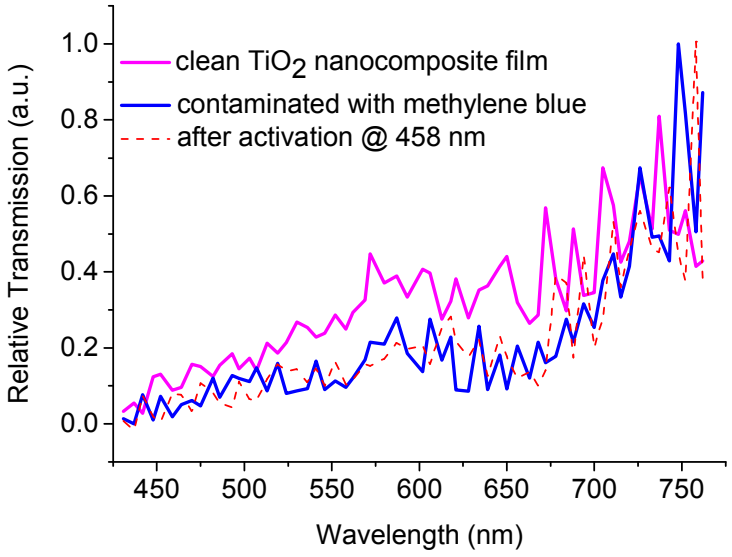
clean TiO2 nanocomposite film
contaminated with methylene blue
after activation @ 458 nm
Relative Transmission (a.u.)
Wavelength (nm)
0.0
0.2
0.4
0.6
0.8
1.0
450
500
550
600
650
700
750

(b)

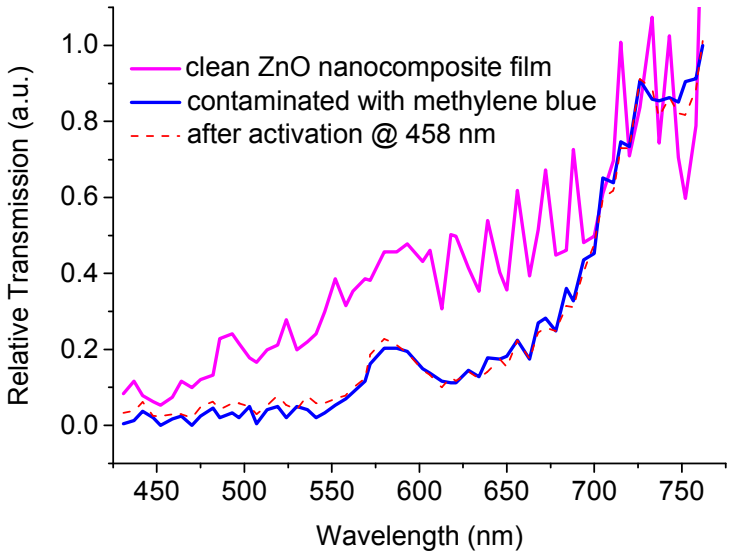

(c)

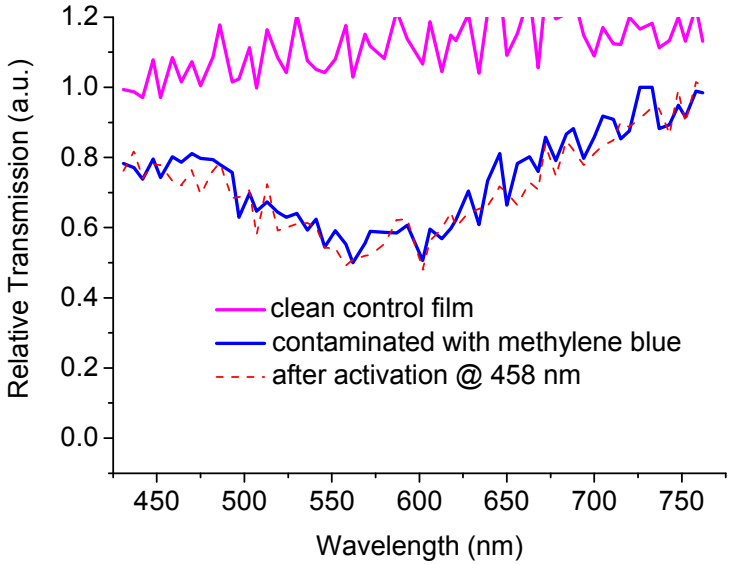

(d)

Figure 3.6.1.10 Optical transmission spectra of the films consisting of (a) TiO_2-ZnO combined nanocomposite, (b) only TiO_2, and (c) only ZnO nanocomposites before and after they are contaminated with methylene blue, and after they are photocatalytically activated at 458 nm keeping the total number of incident activation photons per unit area ([activation power x time] / [spot size x photon energy] constant at 10^{22} m^{-2} along with (d) the host resin without any nanoparticles as the control group.

The control group experiments show that acrylic sol-gel does not degrade significantly in the absence of photocatalyst semiconductors. The optical spectral response of the control group is shown in Fig. 3.6.1.11.

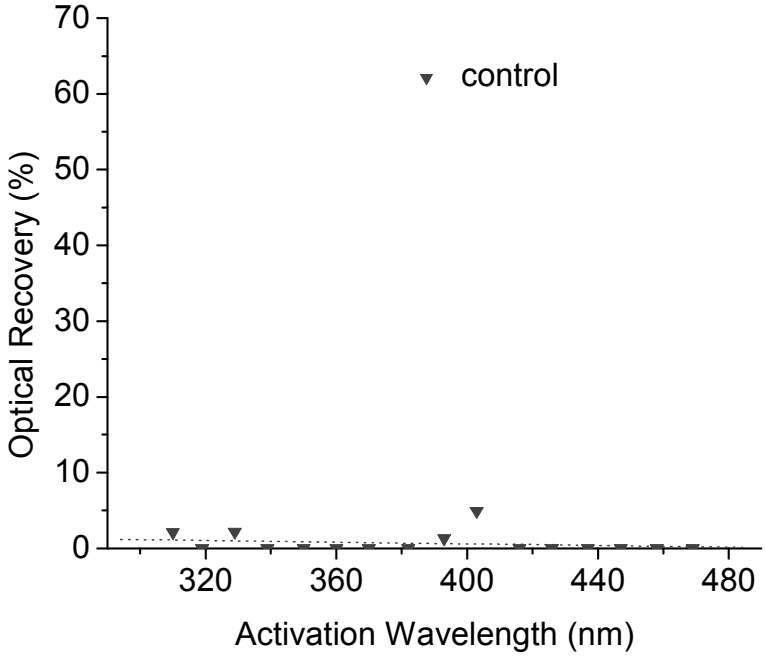

Figure 3.6.1.11 Photocatalytic spectral response of acrylic sol-gel host resin (control).

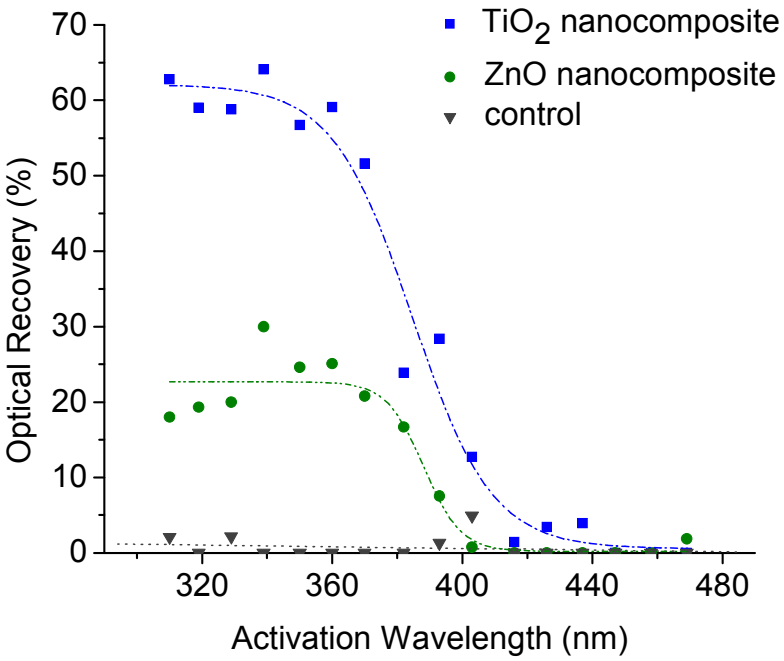

Figure 3.6.1.12 Photocatalytic spectral response of only TiO_2 and only ZnO nanocomposite films.

The optical spectral response of only TiO_2 and only ZnO nanocomposite films are given in the same graph in Fig. 3.6.1.12. The fast decrease in the optical recovery level is at shorter wavelength (~370 nm) for TiO_2 than it is for ZnO (~380 nm). These curves are related with the absorption band edges for these nanocomposite films. Both TiO_2 in anatase form and ZnO have band gap energies of about 3.2 eV. This band gap energy corresponds to the wavelength of ~387 nm. The difference in the absorption edge results from the widening of the bandgap with shrinking size for 6 nm TiO_2 nanoparticles.

Also TiO_2 continues its photocatalytic activity at significant levels when optically activated at wavelengths between 380 nm and ~420 nm. This stems from the band properties of anatase TiO_2 semiconductor. Its absorbance has a tail between 380 nm and ~420 nm [36], also presented in section 3.2. Indirect transitions are allowed at these activation wavelengths [36]. So a significant amount of photocatalytic activity is observed.

3.6.2 Photocatalytic synergy effect of TiO_2-ZnO combined nanocomposite film

Adding the optical recovery data of the combined TiO_2-ZnO nanocomposite film on the previous graph, it becomes clear that combined nanocomposite film has an enhanced photocatalytic activity above 380 nm. Enhanced photocatalysis is achieved both in the near-UV and the visible spectra.

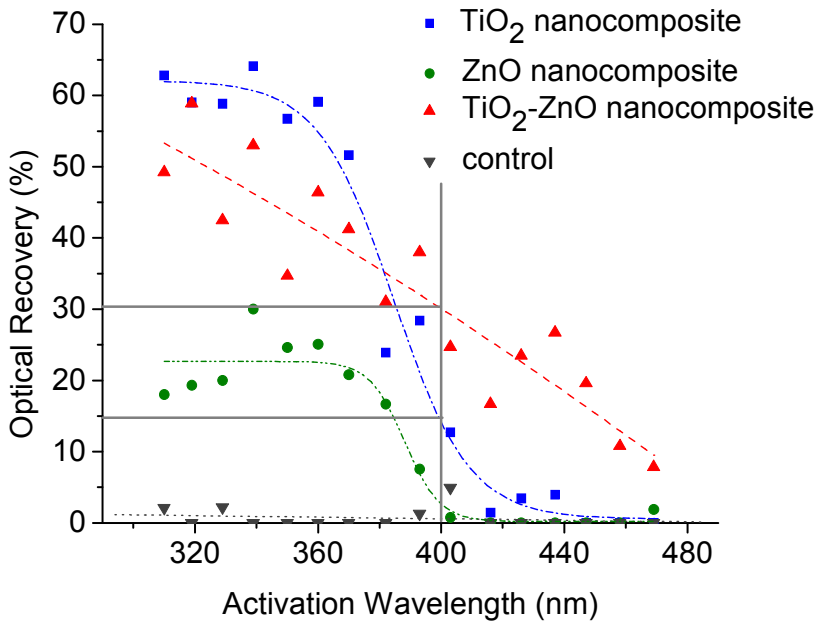

Figure 3.6.2.1 Photocatalytic synergy effect with the use of TiO_2-ZnO combined nanocomposite in the near-UV and the visible activation spectra.

In Fig. 3.6.2.2, the boltzman fit data above 380 nm activation wavelength (where the rates of recovery levels of all three sets are in a tendency to decrease) is shown for the visualization of the enhancement with TiO_2-ZnO nanocomposite film. Despite only TiO_2 and only ZnO films do not show photocatalytic activities at wavelengths as high as 440 nm as expected, TiO_2-ZnO nanocomposite film shows a significant photocatalytic activity at those

wavelengths. Its optical recovery level is ~30% at 400 nm activation wavelength when only TiO_2 film has ~14% and only ZnO film has ~3%. Also at higher wavelengths TiO_2-ZnO nanocomposite film continues its activity. Even at 440 nm activation wavelength; ~20% optical recovery is achieved.

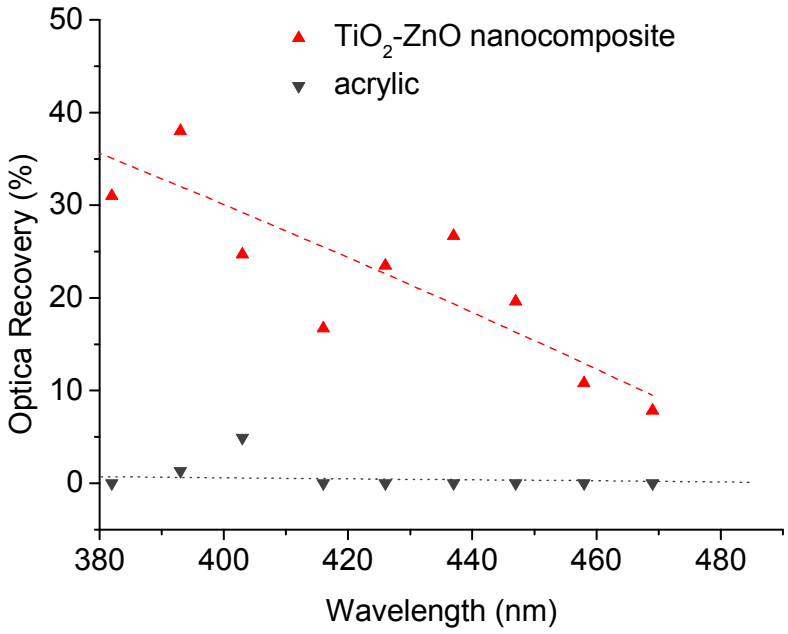

Figure 3.6.2.2 Boltzman fit of optical recoveries after activation in the range from 380 nm to 469 nm.

Chapter 4

Conclusion

In conclusion, we studied photocatalyst nanoparticles chemically integrated inside three dimensional host resins through a homogenous distribution of nanoparticles with a very low number of aggregates and we developed a spectroscopic approach for the characterization of photocatalytic activities of semiconductor metal-oxide nanoparticles for the first time. We achieved very high photocatalytic activities, which is much more difficult with immobilized forms.

For the first time we showed the effect of nanoparticle size on the photocatalytic activities of immobilized nanoparticles through demonstration of widening of the bandgap due to quantum size effect. For the first time, we reported a detailed study on the effect of optical activation wavelength both in the ultraviolet and in the visible. We investigated the photocatalytic spectral response of TiO_2 and ZnO nanocomposite films. We obtained the optimum excitation wavelengths. We presented the photocatalytic activity comparison of TiO_2 and ZnO nanocomposite films. We obtained higher photocatalytic activity and differential photocatalytic activity values for smaller size TiO_2 nanoparticles immobilized in sol-gel film.

The energy band of highly active photocatalytic nanoparticles limits the activation of those photocatalysts in the presence of sunlight. Most commonly used metal-oxides, TiO_2 and ZnO, are wide band gap semiconductors that can be activated only in the UV. We proposed and demonstrated a new method for enhanced photocatalytic activity under sunlight. For the first time, we integrated two different types of wide band gap semiconductors in the same resin, TiO_2 (6 nm in diameter) and ZnO (150 nm in diameter), and achieved enhanced photocatalytic activities at activation wavelengths above ~380 nm. We obtained

significant amount of photocatalytic degradation even in the visible spectrum. Enhanced optical recovery levels due to photocatalytic synergy of TiO_2 and ZnO nanoparticles are promising for the decontamination of large outdoor areas and reducing the NO_x and CO_x amounts in air in daylight. Such highly active immobilized nanoparticles are much more desirable in industrial applications.

CONTRIBUTIONS

[1] S. Tek, E. Mutlugun, I. M. Soganci, N. Kosku Perkgoz, D. Yucel, G. Celiker, and H. V. Demir, "Comparative study of optically activated nanocomposites with photocatalytic TiO_2 and ZnO nanoparticles for massive environmental decontamination," *J. Nanophoton*., vol. 1, 2007.

[2] I. M. Soganci, E. Mutlugun, **S. Tek**, I. O. Huyal, D. Yucel, G. Celiker and H. V. Demir, "The critical role of particle size and spectral activation conditions in the photocatalysis of titanium dioxide nanoparticles," submitted.

[3] S. Tek, D. Yucel, G. Celiker, and H. V. Demir, "Optical spectral activity of immobilized ZnO nanoparticles for photocatalysis," submitted.

[4] S. Tek, N. K. Perkgoz, E. Mutlugun, I. M. Soganci, D. Yucel, G. Celiker and H. V. Demir, "Photocatalytic synergy of TiO_2-ZnO nanocomposites for extending photocatalysis towards the visible," will be submitted. (on hold due to patent application)

[5] S. Tek, H. V. Demir,D. Yucel, and G. Celiker, "Combination of TiO_2-ZnO nanoparticles chemically integrated into acrylic for enhanced photocatalytic activity in the near-UV," *International Symposium on Nanotechnology in Environmental Protection and Pollution (ISNEPP)*, Fort Lauderdale, FL (11-13 December 2007). Paper LT1 14:40.

[6] H. V. Demir, E. Mutlugun, **S. Tek**, S. Nizamoglu, I. M. Soganci, E. Sari, T. Ozel, I. O. Huyal, G. Zengin, and C. Uran, "Functional Nanophotonic Materials for Hybrid Use in Optoelectronics," *2007 Material Science and Technology Conference and Exhibition, Nanostructured Ceramic Materials, Science and Technology Symposium: Functional Behavior and Characterization of Nanomaterials*, Detroit, Michigan (16-20 September 2007). Invited Paper.

[7] H. V. Demir, S. Nizamoglu, E. Mutlugun, T. Ozel, I. M. Soganci, **S. Tek**, I. O. Huyal, E. Sari, G. Zengin, and C. Uran, "Hybrid Nanophotonic Approaches for New Functionality," *SPIE Optics East Conference on Optoelectronic Devices: Physics, Fabrication, and Application)*, Boston, MI (9-12 September 2007). Invited Paper.

[8] S. Tek, H. V. Demir, D. Yucel, and G. Celiker, "High Optical Efficiency of ZnO Nanoparticles," Proceedings of *the Conference on Lasers and Electro-Optics (CLEO Pacific Rim 2007)*, Seoul, Korea (26-31 August 2007). Paper WF3-7.

[9] G. Celiker, D. Yucel, E. Mutlugun, I. M. Soganci, **S. Tek**, and H. V. Demir, "Optical efficiency and NO_X reduction properties of photocatalytic $Ti0_2$ nanoparticles activated in UV," Proceedings of *PRA World 2nd International Nano Hybrid Coatings Conference 'Developments of the Minute' (PRA 2007)*, Brussels, Belgium (7-8 March 2007). Session Nano Materials: testing and applications. Invited Paper. Also reprinted as an invited paper in the journal of Pitture E Vernici in English and Italian; Pitture E Vernici vol. 83, no. 9, p. 26-32 (2007).

[10] E. Mutlugun, I. M. Soganci, **S. Tek**, H. V. Demir, D. Yucel, and G. Celiker, "Optical efficiency of self-cleaning TiO_2 nanoparticles activated in UV," *2007 Nanometa Conference*, Seefeld, Austria (8-11 January 2007).

[11] H. V. Demir, **S. Tek**, E. Mutlugun, I. M. Soganci, D. Yücel, and G. Çeliker, "Photocatalyic TiO_2 nanoparticles with very high spectral efficiencies," Nanobilim ve Nanoteknoloji Konferansı (NANOTR III), Bilkent University, Ankara (11-14 Haziran 2007).

[12] I. M. Soganci, E. Mutlugun, **S. Tek**, H. V. Demir, D. Yucel, and G. Celiker, "Size effect in optical activation of TiO_2 nanoparticles in photocatalytic process," Proceedings of *IEEE Lasers and Electro-Optics Society 2006 Annual Meeting (LEOS 2006)*, Montreal, Canada (29 October – 2 November 2006). Paper WN4.

[13] H. V. Demir, I. M. Soganci, E. Mutlugun, **S. Tek**, and I. O. Huyal, "Photonic devices and systems embedded with nanocrystals for new functionality," Proceedings of *SPIE Optics East*, Boston, MI (1-4 October 2006). Invited paper. 6393-13.

BIBLIOGRAPHY

[1] A. Fujishima and K. Honda, "Electrochemical Photolysis of Water at a Semiconductor Electrode," *Nature*, vol. 238, 1972, pp. 37-38.

[2] T. Kawai and T. Sakata, "Conversion of carbohydrate into hydrogen fuel by a photocatalytic process," *Nature*, vol. 286, 1980, pp. 474-476.

[3] K. Hashimoto, T. Kawai, and T. Sakata, "Photocatalytic Reactions of Hydrocarbons and Fossil Fuels with Water. Hydrogen Production and Oxidation," *J. Phys. Chem.,* vol. 88, 1984, pp. 4083-4088.

[4] L. Kavan, M. Grätzel, S. E. Gilbert, C. Klemenz, and H.J.Scheel, "Electrochemical and Photoelectrochemical Investigation of Single-Crystal Anatase," *J.Am.Chem.Soc.,* vol. 118, no. 28, 1996, pp. 6716-6723.

[5] W. Shangguan, "Hydrogen evolution from water splitting on nanocomposite photocatalysts," *Science and Technology of Advanced Materials*, vol. 8, 2007, pp. 76–81.

[6] J. S. Dalton, P. A. Janes, N. G. Jones, J. A. Nicholson, K. R. Hallam and G. C. Allen, "Photocatalytic oxidation of NO_x gases using TiO_2: a surface spectroscopic approach," *Environmental Pollution,* vol. 120, 2002, pp. 415–422.

[7] F. Zhang, R. Jin, J. Chen, C. Shao, W. Gao, L. Li, and N. Guan, "High photocatalytic activity and selectivity for nitrogen in nitrate reduction on Ag/TiO_2 catalyst with fine silver clusters," *Journal of Catalysis,* vol. 232, 2005, pp. 424–431.

[8] S. Banerjee, J. Gopal, P. Muraleedharan, A. K. Tyagi and B. Raj, "Physics and chemistry of photocatalytic titanium dioxide: Visualization of bactericidal

activity using atomic force microscopy," *Current Science,* vol. 90, 2006, pp. 1378-1383.

[9] A. Hagfeldt and M. Grätzel, "Light-Induced Redox Reactions in Nanocrystalline Systems," *Chem.Rev.*, vol. 95, no. 1, 1995, pp. 49-68.

[10] R. F. Khairutdinov, "Chemistry of semiconductor nanoparticles," *Russ. Chem. Rev.*, vol. 67, no. 2, 1998, pp. 109-122.

[11] Y. Wang and N. Herron, "Nanometer-Sized Semiconductor Clusters: Materials Synthesis, Quantum Size Effects, and Photophysical Properties," *J. Phys. Chem.*, vol. 95. no. 2, 1991, pp. 525-532.

[12] R. Comparelli, P. D. Cozzoli, M. L. Curri, A. Agostiano, G. Mascolo, and G. Lovecchio, "Photocatalytic degradation of methyl-red by immobilized nanoparticles of TiO_2 and ZnO," *Water Science and Technology,* vol. 49, no. 4, 2004, pp. 183-188.

[13] T. Wang, H. Wang, P. Xu, X. Zhao, Y. Liu, and S. Chao, "The effect of properties of semiconductor oxide thin films on photocatalytic decomposition of dyeing waste water," *Thin Solid Films*, vol. 334, 1998, pp. 103-108.

[14] M. Miki-Yoshida, V. Collins-Martinez, P. Amezaga-Madrid, and A. Aguilar-Elguezabal, "Thin films of photocatalytic TiO_2 and ZnO deposited inside a tubing by spray pyrolysis," *Thin Solid Films,* vol. 419, 2002, pp. 60-64.

[15] I. M. Soganci, E. Mutlugun, S. Tek, I. O. Huyal, D. Yucel, G. Celiker, and H. V. Demir, "The critical role of nanoparticle size and spectral activation in the photocatalysis of titanium dioxide nanocomposites," submitted.

[16] S. Tek, E. Mutlugun, I. M. Soganci, N. K. Perkgoz, D. Yucel, G. Celiker, and H. V. Demir, "Comparative study of optically activated nanocomposites with photocatalytic TiO_2 and ZnO nanoparticles for massive environmental decontamination," *J. Nanophoton*., vol. 1, 2007.

[17] D. S. Bhatkhande, V. G. Pangarkar and A. A. Beenackers, "Photocatalytic degradation for environmental applications–a review," *J. Chem. Technol. Biotechnol.,* vol. 77, 2001, pp. 102-116.

[18] T. Sato, K. Masaki, K. Sato, Y. Fujishiro and A. Okuwaki, "Photocatalytic properties of layered hydrous titanium oxide/ CdS-ZnS nanocomposites incorporating CdS-ZnS into the interlayer," *J. Chem. Tech. Biotechnol.,* vol. 67, 1996, pp. 339-344.

[19] Y. Nosaka, and M. A. Fox, "Kinetics for Electron Transfer from Laser-Pulse- Irradiated Colloidal Semiconductors to Adsorbed Methylviologen. Dependence of the Quantum Yield on Incident Pulse Width," *J. Phys. Chem.,* vol. 92, 1988, pp. 1893.

[20] K. Hashimoto, H. Irie, and A. Fujishima, "TiO_2 Photocatalysis: A Historical Overview and Future Prospects," *Japanese Journal of Applied Physics*, vol. 44, no. 12, 2005, pp. 8269-8285.

[21] H. Honda, A. Ishizaki, R. Soma, K. Hashimoto, A. Fujishima, R. Clear, R. Sitzema, and J. Lester, "Application of photocatalytic reactions caused by TiO_2 film to improve the maintenance factor of lighting systems. Author's response," *J. Illum. Eng. Soc*., vol. 27, no. 1, 1998, pp. 42-49.

[22] K. Sunada, Y. Kikuchi, K. Hashimoto, and A. Fujishima, "Bactericidal and Detoxification Thin Film Effects of TiO_2 Photocatalysts," *Environ. Sci. & Tech*., vol. 32, no. 5, 1998, 726-728.

[23] V. Subramanian, V. G. Pangarkar, A. A. C. M. Beenackers, "Photocatalytic degradation of para-hydroxybenzoic acid: Relationship between substrate adsorption and photocatalytic degradation," *Clean Products and Processes,* vol. 2, 2000, pp. 149-156.

[24] T. Noguchi, A. Fujishima, P. Sawunyama, and K. Hashimoto, "Photocatalytic degradation of gaseous formaldehyde using TiO_2 film," *Environ. Sci. & Tech*., vol. 32, no. 23, 1998, 3831-3833.

[25] A. A. Yawalkar, D. S. Bhatkhande, V. G. Pangarkar and A. A ACM Beenackers, "Solar-assisted photochemical and photocatalytic degradation of phenol," *J. of Chem. Technol. and Biotechnol.*, vol. 76, 2001, pp. 363-370.

[26] L. Yang, and Z. Liu, "Study on light intensity in the process of photocatalytic degradation of indoor gaseous formaldehyde for saving energy," *Energy Conversion and Management*, vol. 48, 2007, pp. 882-889.

[27] J. Theurich, M. Lindner, and D. W. Bahnemann, "Photocatalytic Degradation of 4-Chlorophenolin Aerated Aqueous Titanium Dioxide Suspensions: A Kinetic and Mechanistic Study," *Langmuir*, vol. 12, no. 26, 1996, pp. 6368-6376.

[28] S. Tanaka and U. K. Saha, "Effects of pH on photocatalysis of 2,4,6-trichlorophenol in aqueous TiO_2 suspensions," *Water Science and Technology,* vol. 30, no. 9, 1994, pp. 47–57.

[29] Y. Ku, R. Leu, and K. Lee, "Decomposition of 2-chlorophenol in aqueous solution by UV irradiation with the presence of titanium dioxide," *Water Research*, vol. 30, no. 11, 1996, pp. 2569-2578.

[30] J. Yu, X. Zhao, and Q. Zhao, "Effect of surface structure on photocatalytic activity of TiO_2 thin films prepared by sol-gel method," *Thin Solid Films*, vol.379, 2000, pp. 7-14.

[31] M. M. Caldwell, "Plant Life and Ultraviolet Radiation: Some Perspective in the History of the Earth's UV Climate," *BioScience,* vol.29, no. 9, 1979, pp. 520-552.

[32] M. Sasaki, S. Takeshita, M. Sugiura, N. Sudo, Y. Miyake, Y. Furusawa and T. Sakata, "Ground-based observation of biologically active solar ultraviolet-B irradiance at 35 degrees N latitude in Japan," *J. Geomagn. Geoelectr. (Japan)*, vol. 45, 1993, pp. 473-85.

[33] A. L. Stroyuk, A. I. Kryukov, S. Ya. Kuchmii, and V. D. Pokhodenko, "Quantum size effects in semiconductor photocatalysis," *Theoretical and Experimental Chemistry*, vol. 41, no. 4, 2005, pp. 207-228.

[34] S. Yanagida, T. Ogata, A. Shindo, H. Hosokawa, H. Mori, T. Sakata, and Y. Wada, "Semiconductor Photocatalysis: Size Control of Surface-Capped CdS Nanocrystallites and the Quantum Size Effect in Their Photocatalysis," *Bull. Chem. Soc. Jpn.*, vol. 68, no. 3, 1995, pp. 752-758.

[35] A. L. Stroyuk, A. I. Kryukov, S. Ya. Kuchmii, and V. D. Pokhodenko, "Quantum size effects in the photonics of semiconductor nanoparticles," *Theoretical and Experimental Chemistry*, vol. 41, no. 2, 2005, pp. 67-91.

[36] M. Schiavello, Heterogeneous photocatalysis, (John Wiley & Sons, 1997).

[37] S. Sakthivel, B. Neppolian, M. V. Shankar, B. Arabindoo, M. Palanichamy, and V. Murugesan, "Solar photocatalytic degradation of azo dye: comparison of

photocatalytic efficiency of ZnO and TiO_2," *Solar Energy Mater. Solar Cells,* vol. 77, 2003, pp. 65-82.

[38] K. M. Reddy, S. V. Manorama and A. R. Reddy, "Bandgap studies on anatase titanium dioxide nanoparticles," *Materials Chemistry and Physics*, vol. 78, 2002, pp. 239-245.

[39] M. A. Aegerter, and M. Mennig, Sol-gel technologies for glass producers & users, (Kluwer Academic Pub, 2004).

[40] S. H. Lee, S. Pumprueg, B. Moudgil, W. Sigmund, "Inactivation of bacterial endospores by photocatalytic nanocomposites," *Colloids and Surfaces B: Biointerfaces,* vol. 40, no. 2, 2005, pp. 93–98.

[41] T. Deguchi, K. Imai, H. Matsui, M. Iwasaki, H. Tada, and S. Ito, "Rapid electroplating of photocatalytically highly active TiO_2-Zn nanocomposite films on steel," *Journal of Materials,* vol. 36, 2001, pp. 4723 – 4729.

[42] T. Deguchi, K. Imai, M. Iwasaki, H. Tada, and S. Ito, "Photocatalytically highly active nanocomposite films consisting of TiO_2 particles and ZnO whiskers formed on steel plates," *Journal of the Electrochemical Society,* vol. 147, no. 6, 2000, pp. 2263-2267.

[43] Z. Yuan, and L. Zhang, "Synthesis, characterization and photocatalytic activity of $ZnFe_2O_4/TiO_2$ nanocomposite," *J. Mater. Chem.,* vol. 11, 2001, pp. 1265–1268.

[44] N**.** J. Peill and N. R. Hoffmann, "Mathematical Model of a Photocatalytic Fiber-Optic Cable Reactor for Heterogeneous Photocatalysis," *Environ. Sci. Technol.*, vol. 32, no. 3, 1998, pp. 398-404.

[45] K. Okamoto, Y. Yamamoto, and H. Tanaka, "Kinetics of heterogeneous photocatalytic decomposition of phenol over anatase TiO_2 power," *Bull. Chem. Soc. Jpn*., vol. 58, no. 7, 1985, pp. 2015-2022.

[46] J. C. Doliveira, A. S. Ghassan, and P. Pichat, "Photodegradation of 2-and3-chlorophenolin TiO_2 aqueous suspensions," *Environ. Sci. Technol*., vol. 24, no. 7, 1990, pp. 990-996.

[47] D. F. Ollis, E. Pelizzetti, and N. Serpone, "Photocatalyzed destruction of water contaminants," *Environ. Sci. Technol*., vol. 25, no. 9, 1991, pp. 1522-1528.

[48] S. Tek, H. V. Demir, D. Yucel, and G. Celiker, "Combination of TiO_2-ZnO nanoparticles chemically integrated into acrylic for enhanced photocatalytic activity in the near-UV," *International Symposium on Nanotechnology in Environmental Protection and Pollution (ISNEPP)*, Fort Lauderdale, FL (11-13 December 2007). Paper LT1 14:40.

[49] N. Capolla and R. A. Lessard, "Real time bleaching of methylene blue or thionine synthesized gelatin," *Applied Optics*, vol. 30, no. 10, 1991, pp. 1196-1200.

[50] T. Tatsuma, S. Tachibana, T. Miwa, D. A. Tryk, and A. Fujishima, "Remote bleaching of methylene blue by UV-Irradiated TiO_2 in the gas phase," *J. Phys. Chem. B*., vol. 103, no. 38, 1999, pp. 8033-8035.

[51] H. D. Jang, S. K. Kim, and S. J. Kim, "Effect of particle size and phase composition of titanium dioxide nanoparticles on the photocatalytic properties," *Journal of Nanoparticle Research,* vol. 3**,** 2001, pp. 141-147.

[52] R. Wang, K. Hashimoto, A. Fujishima, M. Chikuni, E. Kojima, A. Kitamura, M. Shimohigoshi, and T. Watanabe, "Light-induced amphiphilic surfaces," *Nature,* vol. 388, 1997, pp. 431-432.

[53] R. Wang, K. Hashimoto, A. Fujishima, M. Chikuni, E. Kojima, A. Kitamura, M. Shimohigoshi, and T. Watanabe, "Photogeneration of Highly Amphiphilic TiO_2 surfaces," *Adv. Mater*., vol. 10, no. 2, 1998, pp. 135-138.

[54] G. L. Puma and P. L. Yue, "Effect of the radiation wavelength on the rate of photocatalytic oxidation of organic pollutants," *Ind. Eng. Chem. Res.,* vol. 41, 2002, pp. 5594-5600.

[55] S. Chakrabarti and B. K. Dutta, "Photocatalytic degradation of model textile dyes in wastewater using ZnO as semiconductor catalyst," *Journal of Hazardous Materials,* vol. B112, 2004, pp. 269–278.

[56] G. Mascolo, R. Comparelli, M. L. Curri, G. Lovecchio, A. Lopez, and A. Agostiano, "Photocatalytic degradation of methyl red by TiO_2: Comparison of the efficiency of immobilized nanoparticles versus conventional suspended catalyst," *Journal of Hazardous Materials,* vol. 142, 2007, pp. 130–137.

[57] I. M. Arabatzis, S. Antonaraki, T. Stergiopoulos, A. Hiskia, E. Papaconstantinou, M. C. Bernard, and P. Falaras, "Preparation, characterization and photocatalytic activity of nanocrystalline thin film TiO_2 catalysts towards 3,5-dichlorophenol degradation," *Journal of Photochemistry and Photobiology A: Chemistry,* vol. 149**,** 2002, 237-245.

[58] V. Keller and F. Garin, "Photocatalytic behavior of a new composite ternary system: WO_3/SiC-TiO_2. Effect of the coupling of the semiconductors and oxides in photocatalytic oxidation of methylethylketone in the gas phase," *Catalysis Communications*, vol. 4, 2003, pp. 377-383.